# 1. Introduction

Aluminium is a common industrial metal which is extensively used in many areas due to its particular properties. It is a hard and strong, silvery-white metal and it is not found free in nature. Aluminium is mostly obtained by the Bayer process of refining bauxite. It has low density, is non-toxic, non-magnetic and non-sparkling, has a high thermal conductivity, has excellent corrosion resistance, and can be easily cast, machined and formed. Aluminium and its alloys possess good corrosion resistance by virtue of the impermeable oxide layer that forms spontaneously on the surface and prevents it from reacting with air and water but unfortunately some solutions are definitely corrosive and rapidly attack aluminum and its alloys.

Hydrochloride acid and potassium hydroxide are used for pickling of aluminium and despite resistance to corrosion in a great variety of chemical agents, corrosion will happen in these solutions. Salt solutions of neutral or nearly neutral (pH from ~ 5 to 8.5) solutions of most inorganic salts cause corrosion of aluminum. The rate of attack depends on the specific ions present.

Corrosion of metal is the degradation of materials by electrochemical reactions which destroys economy, depletes resources and causes costly and untimely failures of industrial plants, equipment and components. A recent survey on the costs of corrosion showed that the direct cost of corrosion was $276 billion in the United States for 2002, which is approximately 4% of their Gross National Product (NACE International, 2005). It is observed that corrosion exists everywhere and there is no industry or home where it does not penetrate and it demands a state of readiness for engineers and scientists to combat this problem.

One method of controlling corrosion is use of inhibitors. The selection of inhibitors for use in hydrochloric acid and potassium hydroxide baths for pickling aluminium is of substantial economic importance. Electrochemistry is one of the tools which can be used to assess the effectiveness of corrosion inhibitors for metals and alloys. Over the past thirty years, the use of electrochemical methods for probing corrosion processes has increased to the point that they are an indispensable in the study of corrosion. Methods based on the use of DC polarization and electrochemical impedance (EIS) are presented. The polarization resistance method, when performed properly, enables reliable determinations of instantaneous corrosion rates. Possible sources of error include violating linearity, high solution resistance, fast scans rates or inadequate hold times, parallel redox reactions, and non-uniform current and potential distributions. Electrochemical impedance spectroscopy (EIS) has matured greatly over the past 20 years as a tool in corrosion protection research and has proved to be one of the most useful electrochemical characterization techniques presently available.

EIS uses small periodic signals to perturb an electrode surface and measure an electrochemical response that can be analyzed to gain information on corrosion mechanisms and corrosion kinetics.

The aim of this study is to investigate the inhibition effect of benzene- 1, 2, 4, 5 – tetracarboxylic dianhydride (pyromellitic dianhydride) as a heterocyclic compound on corrosion of pure aluminium in acidic and basic solution by using electrochemical techniques and theoretical work based on quantum chemistry calculations which can predict some molecular parameters directly related to the corrosion inhibition behavior of the chemical compounds.

Thus, after the prediction of these parameters, a correlation between those quantities and the corrosion behavior of similar chemical compounds can be made. The

molecular behavior of corrosion inhibitors of aluminium would be investigated quantum electrochemically via the inhibitors' chemical potential ($\mu$) and the molecular hardness ($\eta$). These quantities will be obtained from density functional theory (DFT) calculations. The calculations would be made for isolated inhibitor molecule.

# 2. Literature review

# PART A

## 2.1 Corrosion definition

The phenomenon of corrosion is as old as the history of metals and earth. The verb "corrode" is derived from the Latin word rodere which means "gnaw". This word entered in 1314 the French language to designate the action of gnawing, progressively wearing away by a chemical effect [1, 2].

Defining "corrosion" is a difficult task, in the past the term "oxidation" was used to indicate what is these days called "corrosion". The former is more accurate definition because corrosion also is an electrochemical reaction during which the metal is oxidized; this usually assumes its transformation into an oxide. However corrosion is a slow, progressive or rapid, undesirable deterioration and destructive attack of a metal's properties by chemical or electrochemical reaction such as its surface aspect, its appearance, or its properties under the influence of the surrounding environment: air and humidity, seawater, organic environments, and various solutions [2, 3].

## 2.2 Consequences of corrosion

The consequences of corrosion are many and varied and the effects of these on the safe, reliable and efficient operations of equipment or structures are often more serious than the simple loss of a mass of metal. The magnitude of corrosion depends on the sensitivity of a specific metal or alloy to a particular environment.

Some of the major harmful effects of corrosion can be summarized as follows:

1) Reduction of metal thickness: Hazards or injuries to people arising from structural failure or breakdown.

2) Loss of time in availability of profile-making industrial equipment.

3) Contamination of fluids in vessels and pipes perforation of vessels and pipe.

4) Mechanical damage to valves, pumps, etc, or blockage Pipe by solid corrosion products.

5) Using of metal prosthetic devices in the body is increasing, such as pins, plates, hipjoints, pacemakers, and other implants. New alloys and better techniques of implantations have been developed, but corrosion continues to create problems [2].

## 2.3 Cost of corrosion

Corrosion of metals has been causing huge losses to the economy of countries. For most of countries the average direct and indirect corrosion costs is around billions of dollars per year, corrosion has a serious impact on defense equipment and it is a serious matter for countries with corrosive environments, especially in the tropical climate with the high humidity. This process affects the metal structures of buildings and bridges, the equipment of chemical and metallurgical plants, river and sea vessels, underground pipelines, and other structures.

In the United States, for instance, corrosion-related losses approach a figure of $100 billion per year, which is almost 5% of the gross national product [2-4]. It is clear that corrosion exists everywhere and the metals need to be protected for durability of the surface aspect against any type of corrosion. There are several ways to prevent corrosion of a metal but using inhibitors can significantly retard corrosion without disruption of a process. The type of inhibitors depends very much to the metal and the corroding medium.

## 2.4 Types of corrosion on aluminium

Without an understanding of corrosion, engineering knowledge is incomplete. In designing of all transport carriers, corrosion behavior of materials must be considered. Materials are very important resources of a country and corrosion is a threat for them.

The aim of corrosion studies is to find out how these resources are destroyed by corrosion and how they must be preserved by applying corrosion protection technology.

Aluminium is one of the metals that can be affected by corrosion. The types of corrosion are mostly uniform (generalized) and pitting corrosion and therefore only will be discussed as follows.

### 2.4.1Uniform corrosion

With aluminium this type of corrosion develops as very small pits (in the order of a micrometer) and results in a uniform and continuous decrease in thickness over the entire surface area of the metal. Uniform corrosion is observed mostly in highly acidic or alkaline media, in these media the solubility of the natural oxide film is high and the greater than its rate of formation [2, 3].

### 2.4.2 Pitting corrosion

This is a form of corrosion where irregular shaped cavities on the surface of the metal are formed. Pits usually have no crystallographic shape and their diameter and depth depend on several parameters related to the metal, the medium and service conditions [5, 6].

This is observed in aqueous media close to neutral pH. The corrosion pits are covered with white, voluminous and gelatinous pustules of alumina gel $Al(OH)_3$. It is a complex phenomenon and a major type of failure in chemical processing industry.

## 2.5 Pourbaix diagrams

Pourbaix diagrams or Potential-pH diagrams represent the stability of a metal as a function of potential and pH (**Figure 2.1**). It is one of the most important contributions to the corrosion literature for the behavior of metals in aqueous solutions. At a particular temperature and composition and also at a particular combination of pH and potential, a stable phase can be determined from the Pourbaix diagram. These diagrams are constructed from calculations based on Nernst equations and the redox potential E vs. SHE plotted on the vertical axis and the pH on the horizontal axis.

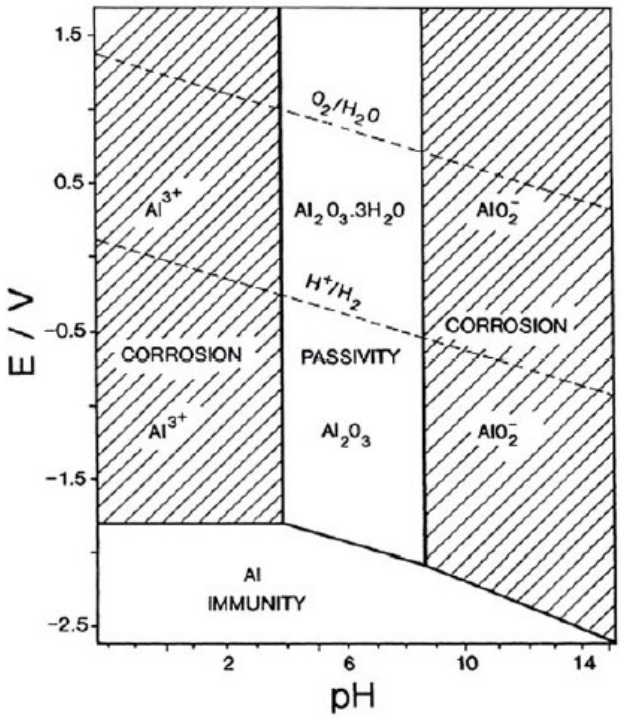


**Figure 2.1** Potential-pH diagram for aluminum [7]

The diagram shows three possible situations: corrosion, passivation and immunity:

– Corrosion Region, products are soluble and have a concentration of $10^{-6}$ M (which amounts to 0.027 $mg \cdot l^{-1}$ for aluminium) as a lower threshold above which it can be assumed that corrosion takes place.

– Passivation region, when an insoluble oxide or hydroxide is formed on the metals surface would not allow corrosion to proceed.

– Immunity region, the concentration of $M^{n+}$ ions is less than $10^{-6}$ M.

The E–pH diagram of aluminium illustrates the amphoteric nature of aluminium: In neutral solutions (pH 4 - 8), the hydroxide is insoluble which makes aluminum surface passive. But it is attacked both in acidic and alkaline media [7].

The thermodynamic information in Pourbaix diagrams can be used to control corrosion of pure metals in the aqueous environment. Unfortunately these diagrams are limited and purely based on thermodynamic data; there is not any information about the rates and kinetics of the reaction. They refer to equilibrium conditions in specified environment and factors. Pourbaix diagrams deal with pure metals and never to an alloy. They do not take into account the role of chloride ions in pitting corrosion and the risk of cathodic corrosion in high electronegative potential [8].

Then it is necessary to use methods such as electrochemical Impedance spectroscopy and potentiodynamic polarization to gather more information about the kinetics of corrosion reactions.

## 2.6 The advantages of aluminium

Aluminium due to its good working and forming properties such as low density, lightness, good appearance, ease of recycling low mechanical strength, high ductility and corrosion resistance is the most applicable metal in the transport power transmission and the metallurgy of non ferrous metals [3, 9]. The production of aluminium has been increasing since 1950 [3] and its corrosion behaviour in different aqueous solutions has attracted the attention of several investigators [4, 8, 10 and 11].

The standard electrode potential of aluminium with respect to hydrogen electrode is -1.66 V but it behaves as a stable metal and is highly resistant to most atmospheres and to a great variety of chemical agents. This is due to the protective oxide film on freshly exposed metal [5]. The pH is one of the parameters that can be used to study the effectiveness on oxide film and the solubility of the oxide film increases above pH 9 and below pH 4 [12, 13].

Acidic and alkaline treatments of aluminium are very important in chemical industry and performed under standard operating conditions for pickling, oil-well acidizing, petrochemical processes, chemical and electrochemical etching of aluminium [14-18].

One of the most effective and inexpensive ways to reduce the corrosion of metal, prevent metal dissolution and minimize acid and base consumption is adding compounds which can reduce the corrosion rate. These compounds when added in small amounts are called inhibitors. These are organic compounds that consist of nitrogen, sulphur or oxygen atoms that the adsorption of these compounds on the metal surface can markedly reduce the corrosion rate of the metal. The inhibitory attributes of these compounds has attracted the attention of many investigators due to the cost saving measures in industry [19-33].

## 2.7 Aluminium corrosion in hydrochloric acid media

Hydrochloric acid (HCl) is one of the most commonly used acids in the pickling or electrochemical etching of aluminium because of its performance and economical advantages. This acid is strong and one of the most aggressive chemicals towards aluminium and aluminium alloys [3]. With increasing aluminium content the rate of dissolution for grades of the 1000 series decreases and the dissolution rate increases with temperature **(Table 2.1)**.

Aluminum corrosion resistance arises from its ability to form a natural oxide film on its surface in a wide variety of media and it has been observed that the oxide film can readily undergo corrosion reactions in chloride environments [34–37].

Oxide film is colourless and built up from two layers with a total thickness between 4 and 10 nm. The first layer is called the barrier layer and in contact with the metal. It is compact and amorphous and forms very quickly after forming or machining operations have destroyed the natural oxide layer locally. The formation rate is independent of the oxygen partial pressure [38, 39].

The maximum thickness of this first layer is in the order of 4 nm [40]. The second layer grows on top of the barrier layer. Its thickness depends on the physicochemical conditions [41]. The second film is porous and less compact than the first one. The composition of its surface is complex and that needs to regenerate by pickling, before any surface treatments.

The composition of the second layer surface is a mixture of $Al_2O_3$ and $Al(OH)_3$ (bayerite) or AlO(OH) (boehmite) and the presence of AlO(OH) is shown by X-Ray. The first layer oxide film composition is in the form of $Al_2O_3$ which is connected to AlO(OH) groups [42].

The corrosion mechanism of aluminum in chloride solutions has been investigated in a number of studies [43- 48]. Various mechanisms have been proposed to explain the breakdown of the passive film [49]. One of them takes into account the migration of chloride ions through the film. Breakdown occurs when chlorides reach the metal–film interface. Recently, one report has shown that the chloride ion does not enter the oxide film instead that it is chemisorbed onto the oxide surface and acts as a reaction partner, aiding dissolution via the formation of oxide–chloride complexes [50].

One important mechanism for the dissolution of Al metal in hydrochloric acid is suggested by Oguzie et al [51].

$$Al_{(s)} + H_2O \rightleftharpoons AlOH_{(ads)} + H^+ + e^- \quad \textbf{(2.1)}$$

$$AlOH_{(ads)} + 5H_2O + H^+ \rightleftharpoons Al^{3+}.6H_2O + 2e^- \quad \textbf{(2.2)}$$

$$Al^{3+} + H_2O \rightleftharpoons [AlOH]^{2+} + H^+ \quad \textbf{(2.3)}$$

$$[AlOH]^{+2} + X^- \rightleftharpoons [AlOHX]^+ \quad \textbf{(2.4)}$$

The limiting step in the metal dissolution is the complexation reaction between the hydrated cation and the anion ($X^-$). In the presence of chloride ions, the corresponding reaction is:

$$[AlOH\ ]^{+2} + Cl^- \rightleftharpoons [AlOHCl]^+ \quad \textbf{(2.5)}$$

Another mechanism is suggested by Awady et al [52]. In this mechanism, aluminium anodic dissolution will be according to the reaction:

$$Al + Cl^- \rightleftharpoons AlCl^-_{(ads)} \qquad \textbf{(2.6)}$$

$$AlCl^-_{(ads)} + Cl^- \xrightarrow{k_1} AlCl_2^+ + 3e^- \qquad \textbf{(2.7)}$$

And cathodic reaction is:

$$H^+ + e^- \xrightarrow{fast} H_{(ads)} \qquad \textbf{(2.8)}$$

$$H^+ + H_{(ads)} + e^- \xrightarrow{k_2} H_2 \qquad \textbf{(2.9)}$$

**Table 2.1** Dissolution rate in hydrochloride acid (mm per year) [3]

| | | HCl concentration | | | | |
|---|---|---|---|---|---|---|
| **Alloy** | **Temperature (°C)** | **0.3 M** | **1.6 M** | **3.2 M** | **4.8 M** | **6 M** |
| 1199 | 20 | 0.1 | 0.4 | 2.6 | 7.0 | 27 |
| | 50 | 1.3 | 3.9 | 5.2 | >50 | >50 |
| | 98 | 18.5 | >50 | >50 | >50 | >50 |
| 1100 | 20 | 0.2 | 7.2 | >50 | >50 | >50 |
| | 50 | 5.2 | 16.0 | >50 | >50 | >50 |
| | 98 | >50 | >50 | >50 | >50 | >50 |
| 3103 | 20 | 1.10 | | | | |
| 6082 | 20 | 2.32 | | | | |
| 44100 | 20 | 1.13 | | | | |

## 2.8 Aluminium corrosion in Potassium Hydroxide solution

The type of aluminium corrosion in this solution is uniform corrosion. The dissolution rate of aluminium at a given pH, as it can see in table, depends on the nature of the base and increases with temperature. Putting a piece of aluminium into hot potassium hydroxide solution releases of hydrogen gas resulting from the attack which is a real hazard. In general, the dissolution rate of aluminium alloys depends on the concentrations and can be very high **(Table 2.2).**

**Table 2.2** Dissolution rate of 1050 in potassium hydroxide at 20 °C [3]

| **Concentration ($g \cdot l^{-1}$)** | **pH** | **Mass loss ($g \cdot m^{-2} \cdot h^{-1}$)** | **Dissolution rate ($mm \cdot h^{-1}$)** |
|---|---|---|---|
| 0.01 | 10.4 | 0.0 | 0.0 |
| 0.1 | 11.4 | 2.2 | 0.001 |
| 1 | 12.4 | 8.5 | 0.003 |
| 10 | 13.2 | 30.0 | 0.01 |
| 50 | 13.7 | 61.5 | 0.02 |

Some pickling baths are based on potassium hydroxide; it is used for pickling before surface treatments of pieces in aluminium alloy. This process has to be carried out under strictly controlled conditions.

For cleaning of aluminium equipments in certain food industries, the addition of sodium or potassium silicate to cleaning solutions is used to stop the attacks on the aluminium.

In the absence of any trace of humidity, potassium hydroxide has no action on aluminium, even above its melting point of 318 ºC [53]. However, the slightest trace of humidity provokes a violent attack on aluminium. For example, the dissolution rate in a eutectic mixture of sodium hydroxide and potassium hydroxide, is 2 $mm \cdot h^{-1}$ with 1% water, but 0.40 $mm \cdot h^{-1}$ with 8.5% water [54].

Mechanism for the dissolution of Al metal in potassium hydroxide can be shown by one of these reactions:

$$Al + KOH + H_2O \longrightarrow KAlO_2 + 3/2\ H_2 \qquad \textbf{(2.10)}$$

$$Al + KOH + 5H_2O \longrightarrow K^+ + (Al(OH)_4.2H_2O)^- + 3/2H_2 \qquad \textbf{(2.11)}$$

## 2.9 Aluminium corrosion in inorganic salts

Inorganic salts result from the reaction of an acid on a base or from the action of an acid on a metal. They are usually solids and white powders at room temperature.

Most soluble inorganic salts are reduced in contact with aluminium in the presence of humidity, taking into account the respective potentials of reduction and oxidation.

### 2.9.1 Sodium Sulphates

Sodium sulphate, $Na_2SO_4$, is used in detergents, paper and glass making. When Sodium sulphate is dry, it has no action on aluminium but it provokes uniform attack of

aluminium at room temperature. The intensity of the attack does not increase with temperature, but superficial pitting occurs at a temperature of 50 $^{o}$C and higher [55].

The $SO_4^{-2}$ ions are bulkier and less mobile than chlorides, they penetrate less easily into the oxide film [56]. Their action on the corrosion resistance of aluminium in water is weaker than that of chlorides. They have a tendency to lead to a significant increase in pitting depth and to inhibit the formation of boehmite layers [57]. As in the case of chlorides, the action of sulphates does not depend on the nature of the associated alkali or earth alkali anion.

### 2.9.2 Sodium Chlorides

Sodium chloride NaCl is a halide salt and extracted from seawater by evaporation or from salt mines and produced in the highest quantity. It has many uses in the food and chemical industries. In presence of NaCl solutions aluminium will suffer a very dense pitting corrosion because of chloride ions [3].

## 2.10 Corrosion inhibitor

The words “inhibit” which means to refrain, to stop, is derived from the Latin word “inhibere”. The word “inhibition” has been used in corrosion science and chemistry since 1907 [58].

Inhibitors are chemical substances that in small concentrations can decrease or prevent the reaction of the metal with the aggressive solutions.

The corrosion resistance of aluminum arises from its ability to form a natural and rapid oxide film on its surface, which is composed of $Al_2O_3$, $Al(OH)_3$ and AlO(OH) phases

in a wide variety of media [36], but the solubility of the oxide film increases above pH 9 and below pH 4 exhibits uniform attack [13, 59-71]. Also aluminum may be used in neutral solutions containing pitting agents such as chloride ions that cause pitting corrosion.

To overcome the detriment of metals and considerable economic losses [72], use of corrosion inhibitors is one of the most effective methods to protect metal surfaces against attack from corrosive media such as chemical cleaning and pickling. Certain organic products can inhibit the action of diluted hydrochloric acid. Most of them are amines, such as aniline, dibutylamine, thiourea, naphthoquinone, acridine, nicotine. Their effectiveness depends on the acid concentration and on the temperature. Their lifetime is limited. Preliminary tests are recommended in order to determine the performance of an inhibitor in a given medium (some examples are given in the next page **(2.10.1)** [73 - 81].

It has been reported that organic substances containing polar groups such as nitrogen, sulphur and oxygen [82-89] as well as heterocyclic compounds containing conjugated double bonds [90 -95] are good inhibitors for metal corrosion.

Despite a large number of organic compounds, there is always a need for developing new organic corrosion inhibitors [96 -98].

As the corrosion of aluminium is an electrochemical reaction with two anodic and cathodic processes, inhibitors can modify the anodic or cathodic reactions, or even both at the same time. Therefore they can be classified to anodic, cathodic and mixed inhibitors:

– anodic inhibitors: They modify the anodic reactions by absorbing on the anodic surface; chromates, nitrites.

– cathodic inhibitors: They modify the cathodic reactions and slow down corrosion by increasing the overpotential of hydrogen ($H^+$) reduction on the cathodic zones [99].

Unfortunately some of inhibitors are toxic and in line with environmental protection requirement, the uses of organic inhibitors is these days are quite limited, so these kind of inhibitors that are widely used in industrial processes should be replaced with new environment friendly inhibitors and conform to standards and regulations concerning toxicity and environmental protection. [100].

### 2.10.1 Examples of applications of inhibitors

Inhibitors are mainly used in the following situations:

– In heat exchangers, like cooling systems of car engines, solar heating, and etc. These are circuits comprising several metals and alloys, therefore all metal need to be protected against corrosion by the coolant, usually water which contains antifreeze additives should contain effective inhibitors [101]. The corrosion of other components may lead to corrosion of the heat exchangers or other aluminium components.

– For surface treatments acidic and alkaline pickling treatments are mostly used; therefore inhibitors are used to minimize the attack of the metal during its short immersion in the pickling bath.

– For degreasing of aluminium equipment used in the food industry, especially in alkaline medium. Using inhibitors are necessary because the blackening by silicates or fluorosilicates cannot be completely prevented [102, 103].

– in the petroleum industry inhibitors are used both in production and refining are either oil soluble-water insoluble types or oil soluble-water dispersible compounds [104].

– inhibitors can also be used in protecting aircraft against corrosion during cleaning operations [105]. Construction industry, feedwater and boiler sections and Sour Gas systems [2, 104].

This shows that inhibitors have wide range of applications in various environments. But they are very rarely used in open systems, because of their cost and environmental problems.

## 2.10.2 Classification of inhibitors

Inhibitors can be classified from their functions into two major classes: inorganic and organic. The anodic type of inorganic inhibitors includes chromates, nitrites, molybdates and phosphates, and the cathodic type includes zinc and polyphosphate inhibitors. The film forming class is the major class of organic inhibitor as it includes amines, amine salts and imidazolines - sodium benzoate mercaptans, esters, amines and ammonia derivatives [2].

These two groups of inhibitors can be classified into two other sub-groups as shown in **Table 2.3** [106]. Most of passivating inhibitors are inorganic oxidants such as chromates, molybdates, chromates and nitrates; they tend to passify the metal surface. [107 - 111].

In the presence of these inhibitors, the potential of the metal shifts to noble regions and metal will be protected. Non-passivating inhibitors such as $Mg^{+2}$ and $Ca^{+2}$ ions in alkaline solutions would react with the hydroxyl ion and precipitate insoluble compounds which would passivate the cathodic zone of the metal. Others include phosphates and polyphosphates which may form a very thin passive film on the metallic surface and suppress corrosion.

Most organic inhibitors contain a polar molecule that creates a physical or chemical covalent bonding with the metal. They include non-volatile and volatile inhibitors. The former is used in acidic and alkaline solutions, metals treatments and the latter is also

called vapor phase inhibitor, used in machinery, components, equipment and packing crates during transportation by sea [106].

**Table 2.3** Classification of inhibitors

| **inorganic inhibitors** | | **organic inhibitors** | |
|---|---|---|---|
| **passivating** | **nonpassivating** | **nonvolatile** | **volatile** |
| Oxidants those are easy to reduce, such as chromates, molybdates, chromates and nitrates. | $Mg^{+2}$, $Ca^{+2}$ ions, phosphates, polyphosphates. | They are used in acidic and alkaline solutions. | They are transported to the desired site by volatilization from a given source. They also extend the protection offered by VPI-impregnated wrapping papers to areas out of contact with the wrapping papers so that protection may be achieved by the areas where wrap cannot be applied to complex shapes of the component. |

### 2.10.3 Parameters influencing the inhibitors efficiency

Some conditions and factors affect the inhibitors' ability and effectiveness towards corrosion protection such as [112-116].

- temperature: adsorption decreases with increasing temperature.
- the type and number of bonding atom or polar groups in the molecule.

– the inhibitor's concentration and chemical structure. (The planarity and the presence of a lone pair of electrons on the heteroatoms).

– strength of bonding to metal substrate.

– the surface charge and the nature of the metal.

– the mode of adsorption of the inhibitor.

– the type of corroding medium.

Organic compounds as inhibitor have the highest efficiency among all compounds. Despite the large number of organic compounds, there is always a need for developing new organic corrosion inhibitors [117, 118].

### 2.10.4 Mechanism of inhibition

The mechanism of inhibition has been the subject of many hypothesis and is still rather poorly understood [119].

The first stage of the mechanism of the organic inhibitors is adsorption on the metal surface, where this process is formed. In chemisorption, bonds are formed between the inhibitors and the metal surface which can prevent corrosion.

There are two kinds of adsorption which can happen:

1) Physical adsorption (physisorption)

2) Chemical adsorption (chemisorption)

The inhibitor molecules are bonded to the metal surface by chemisorption, physisorption or complexation [120], with the polar groups acting as the reactive centers in the molecules.

### 2.10.4.1 Physical adsorption

Physical adsorption is caused by electrostatic or Van der Waals forces which exist between the inhibitor (ionic or neutral) and the charged metal surface. In this process, desorption may take place under adverse conditions, like increasing of temperature or velocity [121,122].

### 2.10.4.2 Chemical adsorption

Chemical adsorption (chemisorption) is an irreversible formation of a covalent bonding between the metal and the inhibitor and leads to inhibition of the anodic reaction [121,122]. Characterizations of Physical and Chemical adsorption is listed in **Table 2.4.**

It has been reported that the inhibition efficiency (IE %) of heterocyclic organic compounds follows the sequence: [123-125].

$$O_2 < N_2 < S < P$$

The metal surface is mostly covered by the adsorbed water molecules on adsorption. The inhibitors react by replacing water molecules by organic inhibitor molecules:

$$Org_{(sol)} + nH_2O_{ads} \longrightarrow Org_{ads} + nH_2O_{(sol)} \qquad \textbf{(2.12)}$$

n indicates the number of molecules which are replaced by the inhibitor molecule.

**Table 2.4** Characterizations of Physical and Chemical adsorption

| **Property** | **Physisorption** | **Chemisorption** |
|---|---|---|
| Reversibility | Adsorbed species can easily be removed from the surface by physical force. | In most cases is permanent and irreversible. |
| Energy (Ea) | > 10 Kcal | < 10 Kcal |
| Kinetic | Adsorption is fast and independent of temperature | It is slow and $E_a$ < 6 Kcal |
| Type of forces | Electrostatic or Van der Waals forces | Covalent bonding |

## 2.11 Corrosion studies using linear sweep voltammetry (LSV), electrochemical impedance spectroscopy (EIS) and Scanning electron microscopy (SEM)

### 2.11.1 Introduction

With electrochemical techniques, electrochemical process of metallic corrosion can be studied. During the past several decades many electrochemical techniques have been developed for investigating the causes and mechanism of corrosion process.

These techniques have some limitations but they are very rapid. The application of these techniques is to determine the electrochemical parameters such as corrosion current density, anodic and cathodic Tafel slopes and the corrosion rate [126].

### 2.11.2 Polarization method

The polarization resistance method, based on electrochemical method, enables the determination of instantaneous interfacial reaction rates such as corrosion rates and exchange current densities from a single experiment. The measurement of corrosion rate is equivalent to determination of the kinetics of the corrosion electrochemical process. The fundamental formula for describing the kinetics of an electrochemical reaction is the

Butler - Volmer equation.

### 2.11.2.1 The Butler - Volmer equation

The oxidation and the reduction process of corrosion according to the mixed-potential theory, occur simultaneously at the metal/electrolyte interface without any net electrical charge accumulation. In this case the net measurable current is zero; therefore the corrosion current can not be measured directly.

A perturbation of the corroding electrode by externally imposed polarization potential for determining electrochemical corrosion kinetics is needed to shift the corrosion system from the corrosion potential ($E_{corr}$).

The Butler - Volmer equation can be applied if the cathodic and anodic reactions on the working electrode are kinetic-controlled and the potential is far away from the equilibrium potentials of the individual anodic and cathodic reactions:

$$i = i_{corr}[\exp(\frac{\alpha nF}{RT}\eta) - \exp(\frac{-\beta n' F}{RT}\eta)] \qquad \textbf{(2.13)}$$

Where the $\eta$ is the overpotential, $F$ is Faraday's constant, $R$ is the gas constant, $i$ is the measured current density, $i_{corr}$ is the corrosion current density, $\alpha$ and $\beta$ are coefficients related to the potential drop through the electrochemical double layer, $n$ and $n'$ are the number of electrons transferred in the anodic and cathodic reactions and $T$ is the absolute temperature. This equation is the fundamental formula but it has to be simplified in its practical application to calculate the electrochemical corrosion current. The most commonly used simplified form of the equation is the Tafel equation.

### 2.11.2.2 The Tafel equation

Tafel found this equation empirically in 1905. It can be deduced from equation (2.13) for sufficiently high values of the applied potential:

For anodic polarization, when $\eta >> RT/\beta n'F$ , the following equations are obtained.

$$i = i_{corr}[\exp(\frac{\alpha nF}{RT}\eta)] \qquad \textbf{(2.14)}$$

or

$$\eta = -\frac{2.3RT}{\alpha F}\log i_{corr} + \frac{2.3RT}{\alpha F}\log i \qquad \textbf{(2.15)}$$

Or, for cathodic polarization, when $-\eta >> RT/\alpha nF$

$$i = i_{corr}[\exp(\frac{-\beta n'F}{RT}\eta)] \qquad \textbf{(2.16)}$$

$$-\eta = -\frac{2.3RT}{\beta F}\log i_{corr} + \frac{2.3RT}{\beta F}\log i \qquad \textbf{(2.17)}$$

The equations (2.15) and (2.17) have form the Tafel equation:

$$|\eta| = a + b\log i \qquad \textbf{(2.18)}$$

Where *a* and *b* are Tafel constant.

For anodic polarization:

$$a = -\frac{2.3RT}{\alpha F}\log i_{corr} \text{ and } b = \frac{2.3RT}{\alpha F} \quad \textbf{(2.19)}$$

For cathodic polarization:

$$a = -\frac{2.3RT}{\beta F}\log i_{corr} \text{ and } b = \frac{2.3RT}{\beta F} \quad \textbf{(2.20)}$$

**Figure 2.2** shows a partial polarization diagram and related kinetic parameters.

This diagram allows the determination of the corrosion point where both the hydrogen cathodic and the metal anodic lines intercept**.**

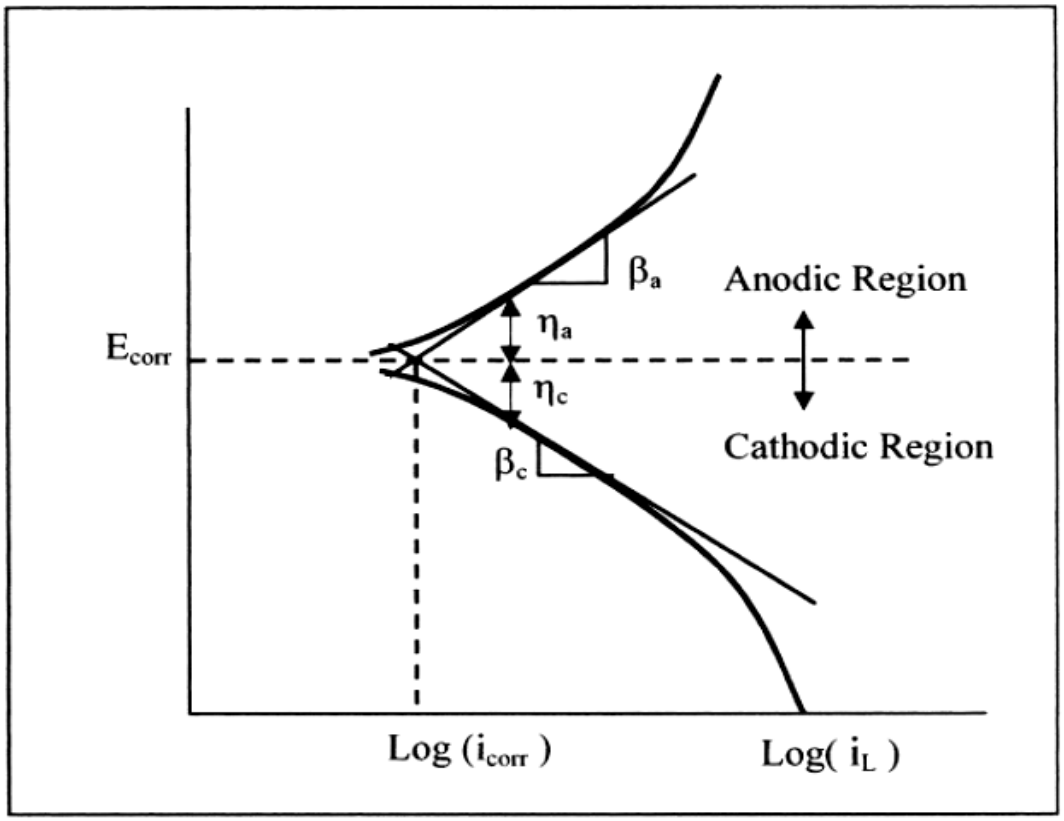

**Figure 2.2** Schematic polarization curve showing Tafel extrapolation.

## 2.11.3 Electrochemical impedance spectroscopy

The electrochemical impedance spectroscopy (EIS) method is very useful in characterizing an electrode corrosion behavior.

The electrode characterization includes the determination of the polarization resistance ($R_p$) corrosion rate ($CR$) and electrochemical mechanism [1, 4, 6, and 21].

The EIS technique is based on a transient response of an equivalent circuit for an electrode/solution interface. The response can be analyzed by transfer functions due to an applied small-amplitude potential excitation at varying signals or sweep rates [126].

### 2.11.3.1 Using EIS in corrosion studies

In the application of EIS, the corroding system in corrosion studies is perturbed from an initial steady state (the corrosion potential) by a broad band, small amplitude sinusoidal signal.

Impedance is written in the form $Z(j\omega) = Z_{re} - jZ_{im}$, where $j = \sqrt{-1}$.

$Z_{re}$ and $Z_{im}$ are frequency-dependent real and imaginary numbers, often referred to as the real and imaginary components of the impedance respectively, which are related to the magnitude of the impedance and the phase by

$$| Z(j\omega)| = \sqrt{Z_{re}^2} - j\sqrt{Z_{im}^2} \qquad \textbf{(2.21)}$$

$\tan \varphi = - Z_{im} / Z_{re}$, where $\varphi$ is the phase angle.

Another mathematical expression of impedance is

$$Z(j\omega) = |Z|e^{j\varphi} \quad \textbf{(2.22)}$$

These two mathematical forms lead directly to the common methods for display in impedance data: the Nyquist plot ($Z_{im}$ vs. $Z_{re}$) and Bode plots ($log|Z|$ vs. $log\ \omega$ – the Bode modulus plot, and $log\ \varphi$ vs. $log\ \omega$ – the Bode phase plot). The Nyquist plot is usually used because it is clearer as the number of relaxation and their mechanistic implications are often more apparent.

### 2.11.3.2 Ideal corrosion system

**Figure 2.3** shows the electrode impedance Nyquist plot in the simplest case; in which corrosion is uniform and corrosion reactions are charge transfer-controlled.

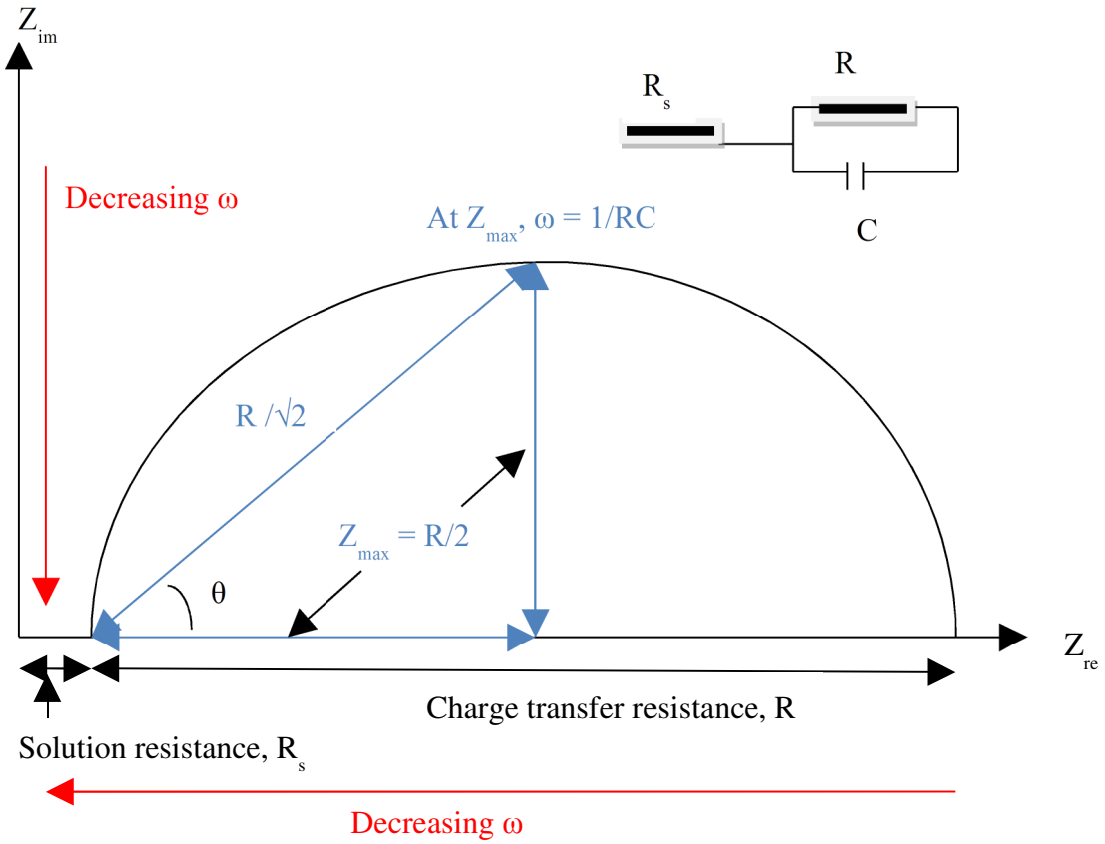

**Figure 2.3** Ideal Nyquist plot of impedance for the electrochemical circuit

The equivalent circuit describes the impedance characteristics. The impedance for this circuit is given by

$$Z(j\omega) = R_{ohm} + R_p/1 + j\omega C_{dl}R_p \quad \textbf{(2.23)}$$

*or,* $$Z(j\omega) = Z_{re} - jZ_{im} \quad \textbf{(2.24)}$$

Where, $$Z_{re} = R_{ohm} + [R_p / 1 + (\omega C_{dl}R_p)^2], \quad \textbf{(2.25)}$$

$$Z_{im} = - [\omega C_{dl}R_p^2 / (1 + (\omega C_{dl}R_p)^2] \quad \textbf{(2.26)}$$

Eliminating the frequency $\omega$ in the equations leads to

$$(Z_{re} - R_{ohm} - R_p/2)^2 + (Z_{im})^2 = (R_p/2)^2 \quad \textbf{(2.27)}$$

$R_{\text{ohm}}$ gives information about solution conductivity; $R_{\text{p}}$ can be related to corrosion rate by the Stern-Geary equation:

$$i_{corr} = (b_a b_c / 2.303(b_a + b_c)) * (1/R_p) \quad \textbf{(2.28)}$$

$C_{dl}$ provide information on adsorption and desorption phenomena, film formation process at the electrode, and the integrity of surface films.

EIS is a reliable technique because it is supposed to be able to separate different corrosion electrochemical processes and eliminate corrosion errors attributed to the solution and surface film resistance.

# PART B

## 2.12 Computational chemistry

### 2.12.1 Introduction

The purpose of computational chemistry is simulation of chemical structures and reactions numerically, based in full or in part on the fundamental laws of physics.
Chemists by running calculations on computers can study chemical phenomena rather than by examining reactions and compounds experimentally.

The most important aspect of computational chemistry is modeling of short-lived, unstable intermediates and even transition states as well as stable molecules. It allows chemists to provide information about molecules and reactions which is impossible to obtain through observation.

Computational chemistry can be an independent area and a vital adjunct to experimental studies; in other words chemists can examine reactions and compounds experimentally and run calculations on computer and then compare results [127].
This chapter provides an introductory overview of computational chemistry, Hohenberg-Kohn theorems and discusses their obvious, Density Functional Theory, the exchange-correlation functional (especiallyB3LYP) and basis sets.

### 2.12.2 Computational chemistry

In computational chemistry devoted to structure of molecules and their reactivity

there are two major areas [127]:

- Molecular mechanics
- Electronic structure theory

They both perform the same basic type of calculations:

1) computing the energy of a particular molecular structure and prediction of properties related to the energy.

2) performing geometry optimizations, which locate the lowest energy molecular structure in close proximity to the specified starting structure. Geometry optimizations depend primarily on the gradient of the energy– the first derivative of the energy with respect to atomic positions.

3) computing the vibrational frequencies of molecules resulting from interatomic motion within the molecule. Frequencies depend on the second derivative of the energy with respect to atomic structure, and frequency calculations may also predict other properties which depend on second derivatives.

### 2.12.3 Molecular Mechanics

Molecular Mechanics simulations by using the laws of classical physics can predict the structure and properties of molecules.

There are many different molecular mechanics methods; each one has its particular force field. A force field has three components:

– The equations that define how the potential energy of a molecule varies with the location of its component atoms.

– Atoms that prescribe different characteristics and behavior for an element depending upon its environment.

– Parameters that fit the equations and atom types to experimental data. They also define force constant; these constants relate atomic characteristic to energy components, and structural data like bond lengths and angles.

Although molecular mechanics computations are quite inexpensive computationally but there are several limitations, such as:

1) Force field cannot be generally used for molecular systems of interest.

2) Molecular mechanics methods cannot treat chemical problems and also reproduction of molecular properties which depend on electronic details is impossible.

### 2.12.4 Electronic structure methods

These methods use the laws of quantum mechanics for their computations. There are two major classes of electronic structures methods:

1) Semi-empirical methods, like AM1, MINDO/3, and PM3, solve an approximate from of the Schrödinger equation.

2) Ab initio methods use no experimental parameters in their computations. Their computations are based solely on the laws of quantum mechanics and only the values of a small number of physical constants:

– The speed of light

1) Planck's constant

2) The mass and charges of electrons and nuclei

Ab initio methods by using rigorous mathematical approximations compute solutions to the Schrödinger equation such as Hartree-fock method (HF), configuration interaction theory (CI), perturbation theory (PT) and coupled cluster (CC).

There are differences in the computational cost and accuracy of results between Semi-empirical and ab initio methods; Semi-empirical calculations are relatively inexpensive and provide good qualitive descriptions of molecular systems and reasonable accurate quantitative predictions of energies and structures for systems where good parameter sets exist; on the other hand, ab initio computations are not limited to any specific class of system and provide high quality quantitative predictions for many systems. Based on supercomputer's specific CPU performance characteristics, it can predict the structures of molecules having as many as one hundred atoms. [127]

There is a third class of electronic structure method which have been used very much; density functional methods. These methods are similar to ab initio methods but they are faster and cheaper than ab initio methods. In recent years, this method has shown high accurate results in catalysis and corrosion inhibition problems [128-133].

### 2.12.5 Density Functional Theory

Thomas and Fermi [134] made a crucial advance towards the resolution of the electronic Hamiltonian in the mid 1920s. They established that the energy of a homogeneous electron gas is a function of its electronic density. Hohenberg and Kohn [135] showed that this principle can be generalized to any kind of electronic system and established the basis of Density Functional Theory (DFT) in 1964. For a system of N electrons and M nuclei, the electronic Hamiltonian can be written as

$$\hat{H} = \hat{T} + \hat{V} + \hat{W} \qquad \textbf{(2.29)}$$

The first term in equation **2.29**, $\hat{T}$ , is the kinetic energy arising from the motion of electrons, the second term are the potential energy of the nuclear-electron attraction, $V$ and the third term is the electron-electron repulsion, $W$.

Hohenberg and Kohn proved that the ground-state molecular energy, wave function, and all other molecular properties are uniquely determined by the exact electron density**,** $\rho$(r).

Therefore, the central focus of DFT is the electronic density, $\rho$, rather than the wave function, $\psi$ .If $N$ is the number of electrons, the density function, $\rho$(r). , is defined by

$$\rho(\vec{r}) = N \int \ldots \int |\psi|^2 \, d\vec{r}_1 d\vec{r}_1 \ldots d\vec{r}_N \qquad \textbf{(2.30)}$$

where $\psi$ is the electronic wave function of the system. Then

$$\int \rho(r)\, dr = N \qquad \textbf{(2.31)}$$

DFT is based on two main theorems, the first and second Hohenberg-Kohn theorems:

*Theorem 1*. The external potential $V$ is a unique functional of $\rho$; since $V$ fixes the Hamiltonian, the particle ground state is a unique functional of $\rho$. Therefore, there is a direct relationship between the electronic density and the energy (and its individual parts).

$$E[\rho] = T[\rho] + V[\rho] + W[\rho] \qquad \textbf{(2.32)}$$

$$V[\rho] = \int \rho(\vec{r})\, v(\vec{r})\, d\vec{r} \qquad \textbf{(2.33)}$$

*Theorem 2*. For a trial density $\rho(r)$, such as $\rho(r) \geq 0$ and $\int \rho(r)\, dr = N$, $E_0[\rho_0] \leq E[\rho]$.

In other words, the energy of the system $E[\rho]$ reaches a minimum value $E_0$ for the exact density $\rho_0$. This is the so-called variational principle.

If we take a closer look at equation **(2.32),** we can separate the $W[\rho]$ functional into two contributions: the classic interaction between two charge densities (Coulomb) and a second term that contains the non-classical parts.

$$W[\rho] = 1/2 \iint [\rho(\vec{r}_1)\rho(\vec{r}_2) / r_{12}] d\vec{r}_1 d\vec{r}_1 + W_{NCL}[\rho] = W_{CL}[\rho] + W_{NCL}[\rho] \qquad \textbf{(2.34)}$$

The complete energy functional can be expressed as

$$E[\rho] = T[\rho] + V[\rho] + W_{CL}[\rho] + W_{NCL}[\rho] \qquad \textbf{(2.35)}$$

In equation (2.35) only the $V[\rho]$ and $W_{CL}[\rho]$ terms are known. To solve the problem of the kinetic energy functional, this term is split into two contributions: $T_s[\rho]$ $T_c[\rho]$. The former is expressed as a one-particle approach (2.36) and the latter, still unknown, contains the difference between the real functional and the one particle term.

$$T_s[\rho] = 1/2\Sigma [\ \psi_i | \nabla^2 | \ \psi_i\ ] \qquad \textbf{(2.36)}$$

Equation (2.36) can be rewritten as follows:

$$E[\rho] = T_s[\rho] + T_c[\rho] + V[\rho] + W_{CL}[\rho] + W_{NCL}[\rho] \qquad \textbf{(2.37)}$$

$$= T_s[\rho] + V[\rho] + W_{CL}[\rho] + E_{XC}[\rho] \qquad \textbf{(2.38)}$$

Where the $E_{xc}[\rho]$ or exchange-correlation functional contains all the unknown terms (all the many-body interactions).

Unfortunately, the Hohenberg and Kohn theorems do not tell us how to calculate $E_0$ from $\rho$ since the exact form of the functional is not known. Kohn and Sham [126,136] invented an indirect approach to this functional. In the Kohn-Sham method, the exact ground state can be found from the Kohn-Sham orbitals,

$$\rho(r) = \sum_{i} | \psi_i(r) |^2 \qquad \textbf{(2.39)}$$

The Kohn-Sham orbitals are obtained from the one-electron Kohn- Sham equations

$$f_s^{KS}\psi_i = \square_i\psi_i \qquad \textbf{(2.40)}$$

where $f_s^{KS}$ is

$$f_s^{KS} = -1/2\nabla^2 - \int[\rho(r_2)/r_{12}]\, dr_2 + \sum_{\mu}[Z_\mu / r_{1\mu}] + v(r) \qquad \textbf{(2.41)}$$

These equations are solved iteratively. Thus, we propose a guess density, which is used to build the $f_s^{KS}$, and then we solve the set of equations **2.41** and obtain a new density, which is used to build a second $f_s^{KS}$, until self-consistency is reached.

No one knows what the exact functional $E_{XC}[\rho]$is. Finding the analytical expression of the exchange-correlation term is a major task in DFT. Some approximate functionals have been proposed.

## 2.12.6 The exchange-correlation functional

To describe $E_{XC}[\rho]$, two approximations are generally used: the *Local Density Approximation* (LDA) and the *Generalized Gradient Approximation* (GGA).LDA is based on a model called uniform electron gas [137]. This approximation assumes that the charge density varies slowly throughout a molecule so that a localized region of the molecule behaves like a uniform electron gas. The exchange- correlation energy is then expressed as a function of the exchange-correlation functional per particle of a uniform electron gas, $\square_{XC}$.

LDA

$$E_{xc}[\rho(r)] = \int \rho(r)\ \varepsilon_{xc}[\rho(r)]\ dr \qquad \textbf{(2.42)}$$

The energy functional accounts for the local value of $\rho$ at each point in space regardless of any other point. Vosko, Wilk and Nusair (VWN) [12] reported the first analytic expression for the correlation term within this approximation.

GGA adds an additional term to the LDA exchange-correlation energy. Gradient corrections are introduced to allow exchange-correlation functional to vary (the density gradient is taken into account). $E_{xc}[\rho(r)]$ is expressed as

$$E_{xc}^{GGA}[\rho(r)] = \int f_{xc}(\rho(r), |\nabla \rho(r)|)\ \rho(r)\ dr \qquad \textbf{(2.43)}$$

There are many exchange-correlation expressions in the literature, e.g. Perdew (P86), Becke (B86, B88), Perdew-Wang (PW91), Laming-Termath-Handy (CAM) and Perdew- Burke-Enzerhof (PBE) for the exchange part and Perdew (P86), Lee- Yang-Parr (LYP), Perdew-Wang (PW91) and Perdew-Burke-Enzerhof (PBE) for the correlation term [138-144].

There is a third class of functionals in DFT called *hybrid functionals*, like the popular B3LYP [14] exchange-correlation functional. These include the exact exchange energy as a contribution from the exact exchange. This approach has extensively proven its accuracy for many systems, although they are more time- demanding than *non-hybrid* exchange correlation functionals because of the calculation of the two-electron integrals in the exact exchange.

In this thesis, the B3LYP method is the method of choice for calculations because of its optimal accuracy.

#### 2.12.6.1 Basis Set

A basis set is a mathematical representation of the molecular orbitals within a molecule. The basis set can be interpreted as restricting each electron to a particular region of space. Larger basis sets impose fewer constraints on electrons and more accurately approximate exact molecular orbitals. They require correspondingly more computational resources.

There are two types of basis functions commonly used in electronic structure calculations: Slater Type Orbitals (STO) and Gaussian Type Orbitals (GTO). Having decided on the type of function (STO/GTO) and the location (nuclei), the most important factor is the number of functions to be used.

Minimum basis set is the smallest number of functions possible. The next improvement of the basis sets is a doubling of all basis functions, producing a Double Zeta (DZ) type basis. The next step up in basis set size is a Triple Zeta (TZ).

STO-nG basis sets are Slater type orbitals consisting of n PGTOs. This is a minimum type basis where the exponents of the PGTO are determined by fitting to the STO, rather than optimizing them by a variational procedure. Although basis sets with n = 2– 6 have been derived, it has been found that using more than three PGTOs for representing the STO gives little improvement, and the STO-3G basis is a widely used minimum basis. This type of basis set has been determined for many elements of the periodic table. The designation of the carbon STO-3G basis is (6s3p) → [2s1p]. 6-311G is a triple split valence basis, where the core orbitals are a contraction of six PGTOs and the

valence split into three functions, represented by three, one and one PGTOs, respectively [127].

# 3. METHODOLOGY

## 3.1 Experimental Section

### 3.1.1 Introduction

Corrosion electrochemical experiments were carried out using AUTOLAB model PGSTAT 30 apparatus and a Pentium IV computer with GPES and FRA softwares.

### 3.1.2 Linear Sweep Voltammetry (LSV)

The polarization curves for the anodic and cathodic reactions are obtained by applying potentials and recording the current. Plotting the logarithms of current (*log i*) vs. potential (*E*) and extrapolating the currents in the two Tafel regions gives the corrosion potential and the corrosion current $i_{corr}$. LSV is the technique which was used and potential was scanned in the range of 350mV to -350 mV with scan rate of 1mV/s.

LSV is one of the most commonly used methods for characterizing corrosion phenomenon. It involves sweeping the potential of the working electrode and measuring

the current response. With LSV it is possible to obtain valuable information regarding the corrosion mechanisms, corrosion rate and susceptibility of specific materials to corrosion in different environments.

### 3.1.3 Impedance spectroscopy (EIS)

The EIS technique has been used successfully to explain corrosion and passivation phenomenon of Al and Al alloys. In addition to specifying the physical properties of the system, the technique leads to important mechanistic and kinetic information.

In this thesis EIS measurements were carried out at the open circuit potential with amplitude of 1 mV in the frequency range from 1 kHz $\leq$ f $\leq$ 0.01 Hz. Potentials were maintained without solution resistance compensation. Impedance-derived solution resistance compensation was, however, performed during data analysis.

The low currents associated with passive region polarizations resulted in a negligible difference between the raw potentials and the IR-compensated potentials.
The impedance data were fit to appropriate equivalent electrical circuit using a complex non-linear least-squares fitting routine, using both the real and imaginary components of the data.

Autolab apparatus includes the working electrode, reference electrode, counter electrode, potentiostat, analyzer generator is shown in **Figure 3.1.**

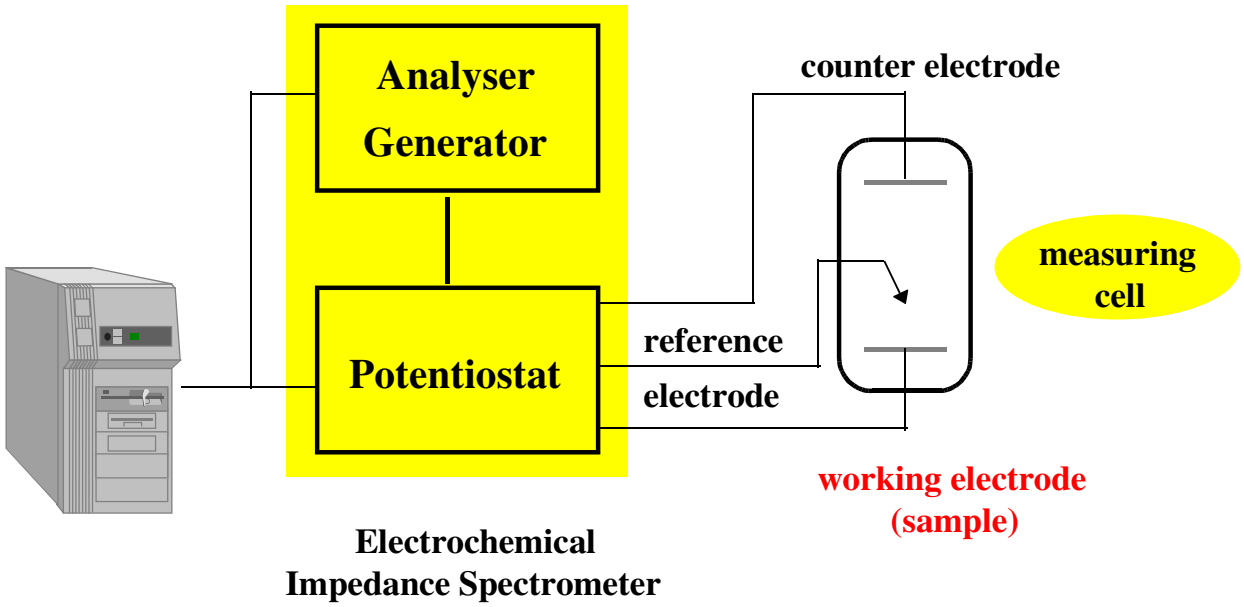


**Figure 3.1** Schematic potentiostat apparatus.

### 3.1.4 Solutions preparation

All electrolyte solutions include HCl (1.0 M), KOH (1.0 M), NaCl (1.0 M) and inhibitor were prepared from Analar, Aldrich, Merck and K&M Chemical companies and with double distilled water.

**• HCl 1.0 M solution**

The aggressive solution of 1.0 M HCl was prepared by dilution of 21.85 ml of concentrated HCl (d = 1.18 g/cm$^3$, $M_w$ = 35.4 g/mol) with doubly distilled water in 250 ml volumetric flask.

**●KOH 1.0 M solution**

By dissolving 11.923 g of KOH (solid, $M_w$ = 56.11g/mol, Purity=85%) in a 250 ml volumetric flask was prepared.

**●NaCl 1.0 M solution**

A NaCl 1.0 M solution by dissolving 14.46 g of NaCl (solid, $M_w$ = 58.44 g/mol, Purity = 99%) in a 250 ml volumetric flask.

**●Stock solution of PMDH 0.1 M**

A stock solution of 0.1 M PMDH ($M_w$ = 218.1222) was prepared by dissolving 5.289 g of PMDH 10% v/v ethanol in water. This addition of ethanol was necessary to dissolve the inhibitor in water, but it does not have any influence on the inhibitive property of the inhibitor, because the water is more nucleophil than ethanol.

### 3.1.5 Electrodes and Cell

In this work a three-electrode cell was used:

1) Working electrode: the pure aluminum rod (99.999%) which the characteristics, preparation and polishing of that will be explained in next section.

2) Reference electrode: The reference electrode is used because its potential is fixed; therefore, any changes in the cell can be ascribed to the working electrode. In this work reference electrode is the saturated calomel electrode (SCE), which is

$$Hg/Hg_2Cl_2/KCl \text{ (saturated in water)} \qquad \textbf{(3.1)}$$

Its potential is 0.242 V vs. NHE.

The distance between the working electrode and SCE in the cell was minimized to reduce the IR drop.

3) Counter electrode: Counter electrode (also called auxiliary electrode) is used to ensure that current does not run through the reference electrode (three electrode system), which would disturb the reference electrode's potential. In this project the platinum counter electrode is used.

### 3.1.5.1 Properties and preparation of working electrode

The working electrode was made of pure aluminum disc. The disc was soldered to Cu wire to provide electrical connection and then was glued with araldite with a hardener using a glass mould. Embedding of Al sample by resin and hardener should be very slow to eliminate air bubbles. The working electrode was left to dry for 24 hours. The working electrode had a surface of 5 mm diameter.

Before each measurement the working electrode was polished with emery papers from 600 to 1200 grits. Then the polished aluminum was immersed in 1.0 M NaOH (etching solution) in 40 $^{o}$C about 30 second to remove the remaining fat traces and the abrasive dust on the electrode surface after polishing, degreased with acetone, washed with doubly-distilled water, and finally dried before being immersed in the solution.

The control of corrosion cell was done by using AUTOLAB model PGSTAT 30 apparatus and a Pentium IV computer with GPES and FRA soft wares.

Experiments were always repeated at least three times until a good reproducibility of the results was obtained.

## 3.2 Computational Section

### 3.2.1 Calculation Method and Chemical Model

In order to predict chemical characteristics in computational chemistry, a chemical model is required for representing information about the chemical system which is under studied.

The chemical model, in fact, is choosing a calculation method and appropriate basis set. Density functional theory (DFT), in particular the hybrid functional B3LYP, is the method of choice in this study. Basis set employed in geometry optimizations is 6-311G (d,p) to describe chemical model.

The Gaussian 03 suite of programs and Gausview 3.0 was used for all calculations in this study. For prediction about the reaction on metal surface, two kinds of calculations were considered by B3LYP: Geometry optimization and Energy.

# 4. Results and discussion

# PART 1

# Electrochemical studies

## 4.1 Effect of Benzene -1, 2, 4, 5-tetracarboxylic dianhydride (PMDH) on aluminum corrosion in 1.0 M hydrochloric acid (HCl) solution

### 4.1.1 Linear polarization method

**Figure 4.1** gives the anodic and cathodic polarization curves of pure aluminium in 1.0 M HCl in the absence and presence of various concentrations of PMDH. It is observed that, both of the cathodic and anodic curves show lower current density in the presence of the PMDH than those recorded in the solution without the inhibitor. This indicates that this inhibitor has an effect on both cathodic and anodic reactions of corrosion process.

Therefore, this compound can be classified as mixed type inhibitor. $E_{corr}$ shifts to more positive values and it indicates that this inhibitor influence anodic region. The electrochemical parameters ($i_{corr}$, $E_{corr}$, $b_c$ and $b_a$) associated with polarization measurements and the inhibitor efficiency *IE%* at different inhibitor concentrations are listed in Tables 4.1, where $i_{corr}$, $b_a$ and $b_c$ are the corrosion current density, anodic and cathodic Tafel slopes, respectively.

The inhibition efficiency (*IE %*) at different inhibitor concentrations and temperatures were calculated from the equation:

$$IE\ \% = \frac{i_{corr} - i_{corr\ (inh)}}{i_{corr}} \times 100 \qquad \textbf{(4.1)}$$

Where $i_{corr}$ and $i_{corr\ (inh)}$ are the corrosion current densities in the absence and presence of the inhibitor.

The results are given in **Table 4.1** reveal that with increasing inhibitor concentration, the corrosion current density and corrosion rate decrease and polarization resistance increases.

The polarization resistance ($R_P$) can be calculated using the Stern – Geary equation:

$$R_p = \frac{b_a.b_c}{2.3(b_a + b_c)\, i_{corr}} \qquad \textbf{(4.2)}$$

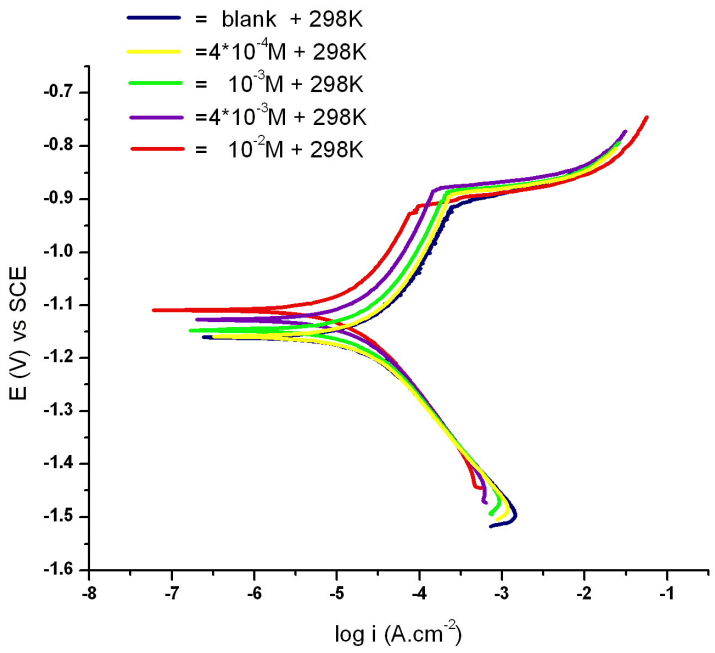


**Figure 4.1** Effect of various concentrations of PMDH in 1.0 M HCl on aluminum polarization curves at 25°C.

**Table 4.1**

Fitting corrosion parameters of aluminum in 1.0 M HCl on the presence and absence of different concentration of PMDH obtained from polarization measurements at 25 °C.

| ***C*** **(M)** | $E_{corr}$ **(mV)** | $b_a$ **(mV/dec)** | $b_c$ **(mV/dec)** | $R_p.A$ **(Ωcm²)** | $i_{corr}/A$ **(μAcm⁻²)** | ***CR*** **(mm/year)** | ***θ*** | ***IE%*** |
|---|---|---|---|---|---|---|---|---|
| Blank | -1160 | 283 | 254 | 1482.08 | 39.40 | 1.29 | — | — |
| 0.01 | -1109 | 330 | 230 | 2596.38 | 22.70 | 0.74 | 0.4238 | 42.38 |
| 0.004 | -1127 | 320 | 229 | 2093.98 | 27.74 | 0.91 | 0.2959 | 29.59 |
| 0.001 | -1149 | 372 | 192 | 1665.18 | 34.10 | 1.1 | 0.1598 | 13.45 |
| 0.0004 | -1159 | 325 | 234 | 1563.52 | 36.87 | 1.24 | 0.04 | 6.4 |

#### 4.1.1.1 Effect of temperature

The effect of temperature on the inhibition efficiency of inhibitor in 1.0 M HCl at temperatures ranging from 25 to 55 °C was obtained to calculate the thermodynamics parameters. **Figure 4.2 (a-e)** shows the effects of different temperatures on the polarization curves of aluminum in 1.0 M HCl in the presence and absence of PMDH.

The results are summarized in **Table 4.2** with increasing temperature, polarization resistance decreases, corrosion current and therefore corrosion rate increases. It can be related to desorption of adsorbed inhibitor' molecules on the aluminum surface and decrease in the strength of adsorption process at higher temperatures. This shows the physical adsorption of the inhibitor molecules on the metal surface.

The effect of PMDH strength on the inhibition efficiency of metal surface is shown in **Figure 4.3** whereas a decrease in the inhibition efficiency (*IE %*) with reducing inhibitor concentration and increasing temperature is observed.

**(a)**

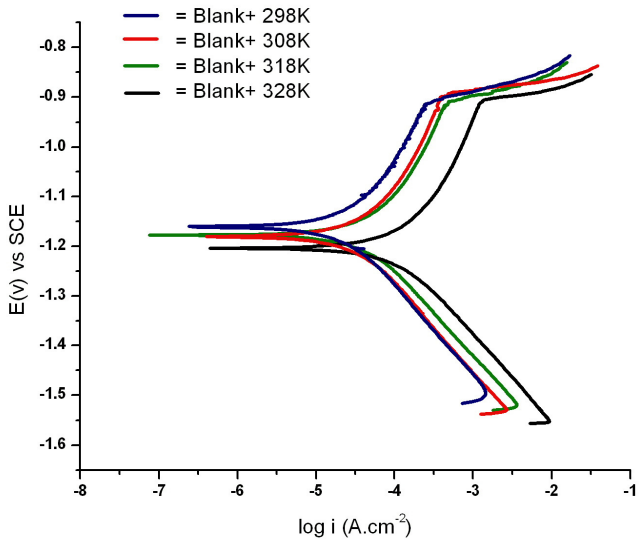

**(b)** **(c)**

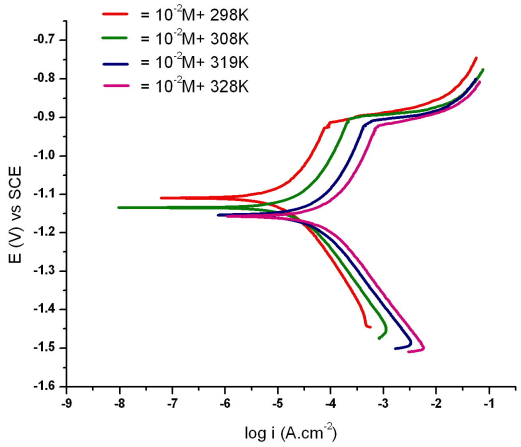
= 10-2M+ 298K
= 10-2M+ 308K
= 10-2M+ 319K
= 10-2M+ 328K
E (V) vs SCE
log i (A.cm-2)

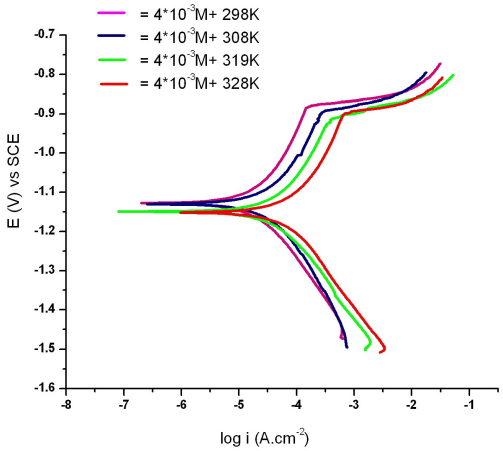
= 4*10-3M+ 298K
= 4*10-3M+ 308K
= 4*10-3M+ 319K
= 4*10-3M+ 328K
E (V) vs SCE
log i (A.cm-2)

**(d)** **(e)**

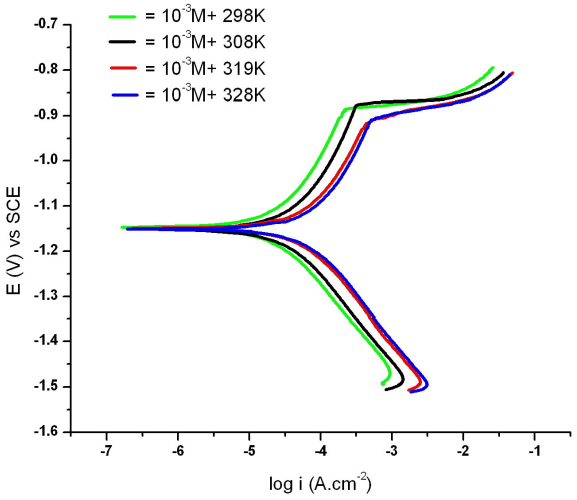
= 10-3M+ 298K
= 10-3M+ 308K
= 10-3M+ 319K
= 10-3M+ 328K
E (V) vs SCE
log i (A.cm-2)

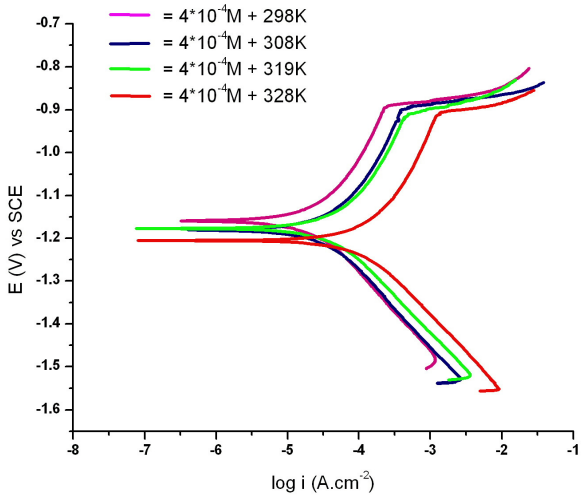
= 4*10-4M + 298K
= 4*10-4M + 308K
= 4*10-4M + 319K
= 4*10-4M + 328K
E (V) vs SCE
log i (A.cm-2)

**Figure 4.2** Polarization curves for Al in 1.0 M HCl in the presence of **(a)** 0.01M PMDH, **(b)** 0.004 M PMDH, **(c)** 0.001 M PMDH, **(e)** 0.0004 M PMDH.

**Table 4.2**

Fitting corrosion parameters of aluminum in 1.0 M HCl on the presence and absence of different concentrations of PMDH obtained from polarization measurements at 25, 35, 45, 55 °C.

| ***C*** | ***T*** | $E_{corr}$ | $b_a$ | $b_c$ | $A.R_p$ | $A.i_{corr}$ | ***CR*** | $\theta$ | ***IE%*** |
|---|---|---|---|---|---|---|---|---|---|
| **(M)** | **(K)** | **(mV)** | **(mV/dec)** | **(mV/dec)** | **($\Omega cm^2$)** | **($\mu Acm^2$)** | **(mm/year)** | | |
| Blank | 298 | -1160 | 283 | 254 | 1482.08 | 39.4 | 1.289 | — | — |
| | 308 | -1177 | 315 | 236 | 1055.23 | 55.7 | 1.824 | — | — |
| | 318 | -1180 | 289 | 214 | 709.21 | 62.9 | 2.598 | — | — |
| | 328 | -1203 | 261 | 195 | 361.49 | 114.6 | 3.546 | — | — |
| 0.01 | 298 | -1109 | 330 | 230 | 2596.38 | 22.7 | 0.74 | 0.4238 | 42.38 |
| | 308 | -1134 | 253 | 203 | 1718.32 | 33.9 | 1.109 | 0.3913 | 39.13 |
| | 318 | -1154 | 244 | 185 | 957.24 | 45.4 | 1.613 | 0.2777 | 27.77 |
| | 328 | -1157 | 195 | 188 | 484.34 | 85.98 | 2.223 | 0.2497 | 24.97 |
| 0.004 | 298 | -1127 | 320 | 229 | 2093.98 | 27.74 | 0.909 | 0.2959 | 29.59 |
| | 308 | -1130 | 324 | 296 | 1357.76 | 44.56 | 1.341 | 0.2179 | 21.79 |
| | 318 | -1149 | 316 | 245 | 837.25 | 53.64 | 1.857 | 0.1466 | 14.66 |
| | 328 | -1151 | 269 | 254 | 405.31 | 102.58 | 2.509 | 0.1048 | 10.48 |
| 0.001 | 298 | -1149 | 372 | 192 | 1665.18 | 34.1 | 1.1 | 0.13 | 13.45 |
| | 308 | -1150 | 286 | 217 | 1140.95 | 51.8 | 1.55 | 0.07 | 7 |
| | 318 | -1151 | 299 | 247 | 749.41 | 59.4 | 2.073 | 0.05 | 5.50 |
| | 328 | -1152 | 344 | 263 | 374.34 | 110.6 | 2.724 | 0.049 | 3.49 |
| 0.0004 | 298 | -1159 | 325 | 234 | 1563.52 | 36.87 | 1.239 | 0.064 | 6. 4 |
| | 308 | -1180 | 293 | 223 | 1095.07 | 54.02 | 1.752 | 0.030 | 3.01 |
| | 318 | -1177 | 288 | 216 | 728.58 | 61.37 | 2.213 | 0.023 | 2.37 |
| | 328 | -1205 | 227 | 179 | 368.51 | 112.3 | 2.939 | 0.020 | 2 |

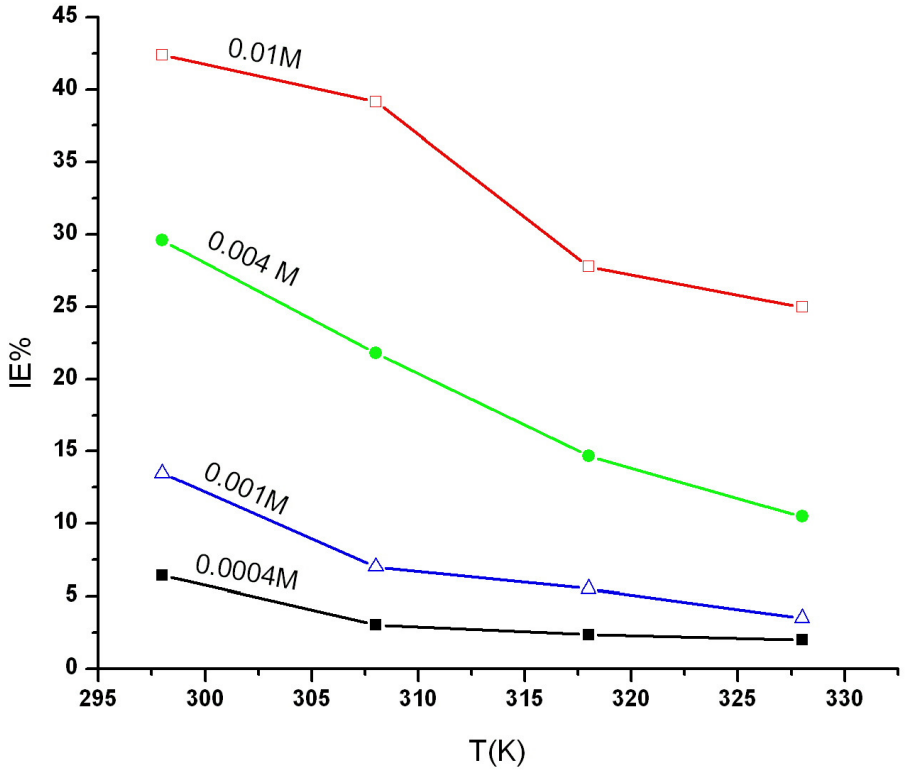


**Figure 4.3** Effect of PMDH on inhibition efficiency of Al corrosion in various concentration and temperatures.

**Figure 4.4** shows the plots of inhibition efficiency (*IE %*) and $R_p$ vs. log *C* in 1.0 M HCl at different temperatures. It is clear that the inhibition efficiency and polarization resistance increases as the concentrations of the inhibitor increase. These results suggest that the inhibitor retards the acid dissolution of aluminum by acid through adsorption in aluminum/acid solution interfacial region.

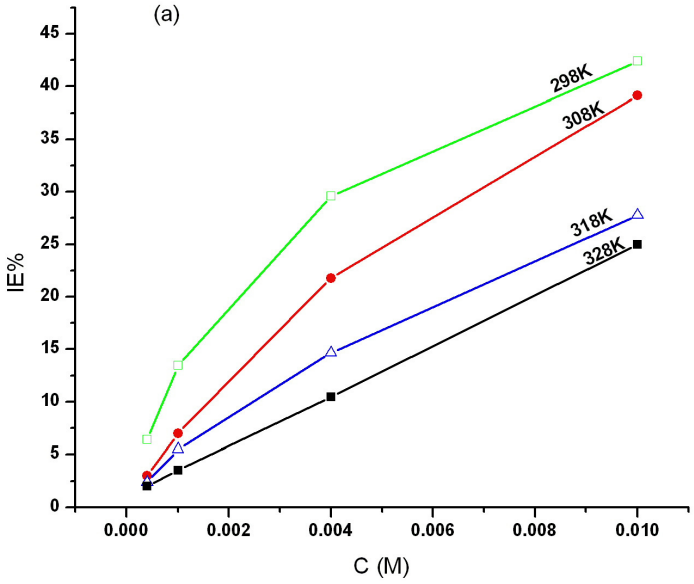
(a)
IE%
C (M)
298K
308K
318K
328K
0
5
10
15
20
25
30
35
40
45
0.000
0.002
0.004
0.006
0.008
0.010

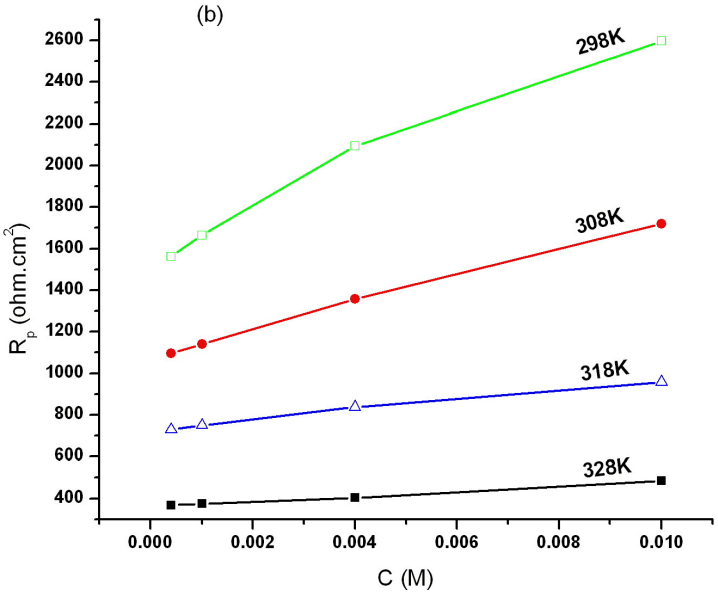
(b)
$R_p$ (ohm.cm$^2$)
C (M)
298K
308K
318K
328K
400
600
800
1000
1200
1400
1600
1800
2000
2200
2400
2600
0.000
0.002
0.004
0.006
0.008
0.010

**Figure 4.4 (a)** Effect of PMDH concentration on inhibition efficiency of Al corrosion in 1.0 M HCl and **(b)** on polarization resistance of Al corrosion in 1.0 M HCL at different temperatures.

### 4.1.1.2 Adsorption isotherm

For the determination of the adsorption process, the values of surface coverage ($\theta$) of different concentrations of PMDH obtained from the polarization measurements in the temperature ranges (25-55 $^{o}$C) have been used.

The metal surface is mostly covered by the adsorbed water molecules on adsorption process. The inhibitor anti–corrosion properties come from the ability to block the charge transfer process on the electrode–electrolyte interphase by replacing the water molecules and ions adsorbed on the electrode surface.

$$Org_{(sol)} + nH_2O_{(ads)} \longrightarrow Org_{(ads)} + nH_2O_{(sol)} \quad \textbf{(4.3)}$$

$$Org_{(sol)} + nH^+_{(ads)} + nCl^-_{(ads)} \rightarrow Org_{(ads)} + nH^+_{(sol)} + nCl^-_{(sol)} \quad \textbf{(4.4)}$$

n indicates the number of molecules which are replaced by the inhibitor molecule, $Org_{(sol)}$ and $Org_{(ads)}$ are the organic molecules in the aqueous solution and adsorbed on the surface of metal, respectively and $H_2O_{ads}$ is the molecules of water adsorbed on the metallic surface.

Among several adsorption isotherms tested for the determination of adsorption behaviour of PMDH on aluminum surface in HCl solution, the best is Langmuir adsorption isotherm which can summarized by:

$\theta$

$$K_{ads} = \frac{\theta}{C_{inh}(1-\theta)} \quad \textbf{(4.5)}$$

where $K_{ads}$ is the equilibrium constants of adsorption process. $C_{inh}$ is the inhibitor concentration, $\theta$ is the surface coverage value. This isotherm assumes that there are no interaction or repulsion forces between the adsorbed molecules. The plot of log ($\theta$/1- $\theta$) versus log C for different concentrations of PMDH in four temperatures is given in **Figure 4.5.**

#### 4.1.1.3 Kinetic-thermodynamic corrosion parameters

The relation between the equilibrium constants of adsorption process ($K_{ads}$) and the free energy of adsorption $\Delta G_{ads}$ is given by the following equation:

$$K = \exp(-\Delta G_{ads}/RT) \quad \textbf{(4.6)}$$

Where R is the universal gas constant and T is the temperature and $\Delta G_{ads}$ is the free energy of adsorption . It is shown that the slope, $K_{ads}$, with an average value of 4082 $dm^3\ mol^{-1}$ is obtained indicating the $\Delta G_{ads}$ = -20.60 kJ $mol^{-1}$. The negative sign and values of free energy for adsorption of PMDH on the metallic surface (less than - 40 kJ/mole) for all concentrations of this inhibitor suggest that the adsorption occurs by physical mechanism and spontaneously.

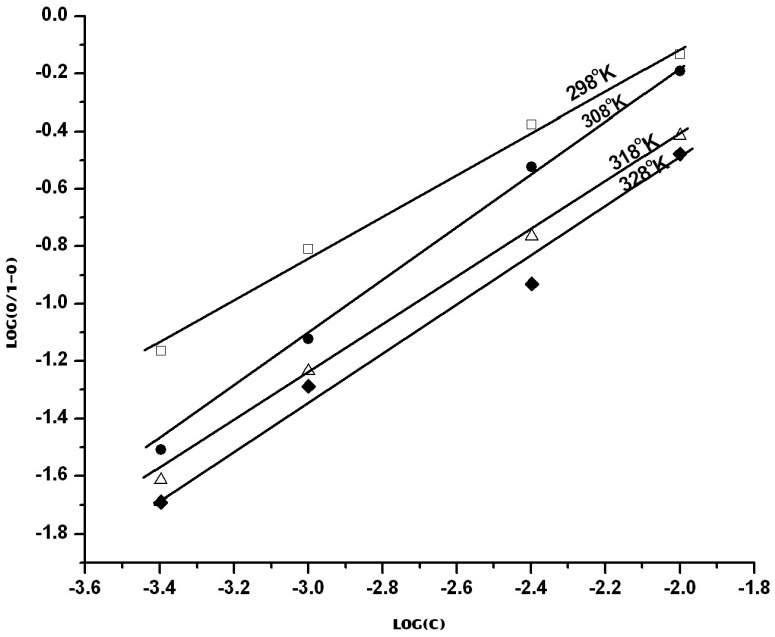


**Figure 4.5** Plot of Langmuir adsorption isotherm of PMDH obtained by using surface coverage values calculated by Tafel polarization in different temperatures.

Activation energies for the aluminum dissolution process can be evaluated from the following relationship [145, 146]:

$$\text{Log (corrosion rate)} = \log A - (E_a/2.303RT) \qquad \textbf{(4.7)}$$

where $A$ plot of log corrosion rate, $E_a$ the activation energy and $T$ is temperature. Plotting log corrosion rate versus $1/T$ gave a straight line with slope of $-E_a/2.303R$ (**Figure 4.6**). It is clear from the results, activation energy decrease in the presence of inhibitor.

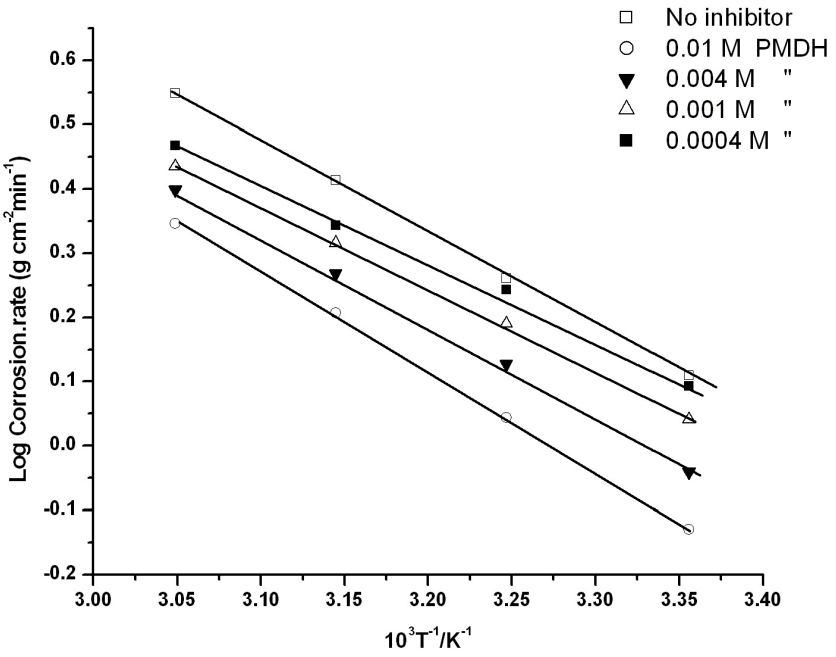


**Figure 4.6** Plotting log corrosion rate vs. 1/T to calculate the activation energy of corrosion process in the presence of inhibitor.

.

The enthalpy of activation ($\Delta H^*$) and the entropy of activation ($\Delta S^*$) for the corrosion of Al in HCl 1M in the absence and presence of different concentrations of PMDH were obtained by applying the transition-state equation [147]:

$$\text{Log (Corrosion. rate / } T) = [(\log(R/hN)) + (\Delta S^* / 2.303R)] - \frac{\Delta H^*}{2.303RT} \qquad \textbf{(4.8)}$$

where $h$ is the Plank's constant and $N$ is the Avogadro's number. A plot of log (corrosion rate/T) Vs 1/T give a straight line with slope of (- $\Delta H^*$/2.303R) and intercept of log [($R/hN$)) + ($\Delta S^*$ /2.303$R$)] from these equations $\Delta H^*$ and $\Delta S^*$ were calculated (**Figure 4.7**).

All thermodynamic results were listed in **Table 4.3**. The values reflect the exothermic behavior of these inhibitors on the Al surface. The negative values of $\Delta S^*$ indicate that, the inhibition process is primarily enthalpy controlled.

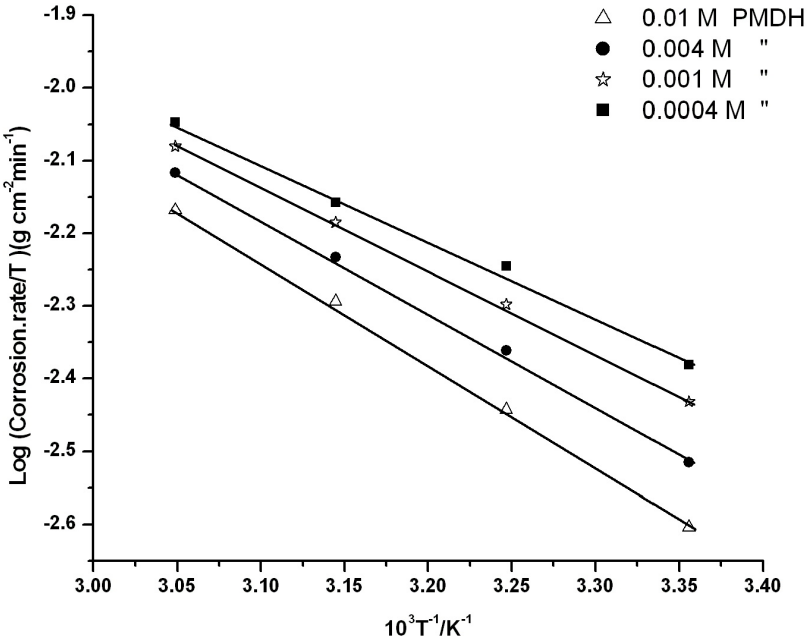


**Figure 4.7** Transition state equation plots of the corrosion reaction in the presence of PMDH.

**Table4.3**

Thermodynamic corrosion parameters for aluminium corrosion in presence of various concentrations of PMDH.

| $C$ (M) | $E_a$ (kJ mol$^{-1}$) | - $\Delta H^*$ (kJ mol$^{-1}$) | $\Delta S^*$(J mol$^{-1}$K$^{-1}$) |
|---|---|---|---|
| 0.01 | 12.963 | 17.92 | - 168 |
| 0.004 | 13.355 | 16.68 | - 170 |
| 0.001 | 14.974 | 14.73 | - 174 |
| 0.0004 | 15.964 | 13.45 | - 176 |

## 4.1.2 Electrochemical impedance spectroscopy

The Nyquist plots for aluminum in 1.0 M HCl solution with and without PMDH in the concentration range of 0.01 to 0.0004 M at 25 °C are shown in **Figure 4.8**.

The impedance parameters calculated from the analysis of these diagrams is given in **Table 4.4.** Values of polarization resistance ($R_p$) were calculated from the difference in impedance at the lower and higher frequencies. Double layer capacitance ($C_{dl}$) was calculated from the maximum imaginary component of the impedance ($-Zi_{max}$) by the following equation:

$$f(-Zi_{max}) = \frac{1}{2\pi C_{dl} R_p} \qquad \textbf{(4.9)}$$

The inhibition efficiency (*IE %*) is calculated by the following equation [148] :

$$(IE\ \%) = \frac{R_{p(inh)} - R_p}{R_{p\,(inh)}} \times 100 \qquad \textbf{(4.10)}$$

where $R_p$ and $R_{p(inh)}$ is the polarization resistance observed in the absence and presence of PMDH. Impedance plots show that the impedance response of aluminum has changed after the introduction of PMDH in 1.0 M HCl. The results indicate that the impedance responses consisted of single capacitive semicircles, showing that the corrosion process was mainly charge-transfer controlled [149]. The high frequency part of the impedance and phase angle describes the behavior of an inhomogeneous surface layer, while the low frequency contribution shows the kinetic response for the charge transfer reaction [150].

By increasing the concentration of inhibitor, the $C_{dl}$ values tended to decrease and the inhibition efficiency (*IE %*) and polarization resistance ($R_p$) were increased. The decrease in the $C_{dl}$ means that adsorption of PMDH molecules at the solution / interface has increased in thickness and conversely, a decrease in local dielectric constant [151]. The data obtained from EIS are in agreement with that obtained from potentiodynamic polarization.

**Figure 4.9** is the circuit diagram generally used to describe the aluminum/acid interface model [152, 153]

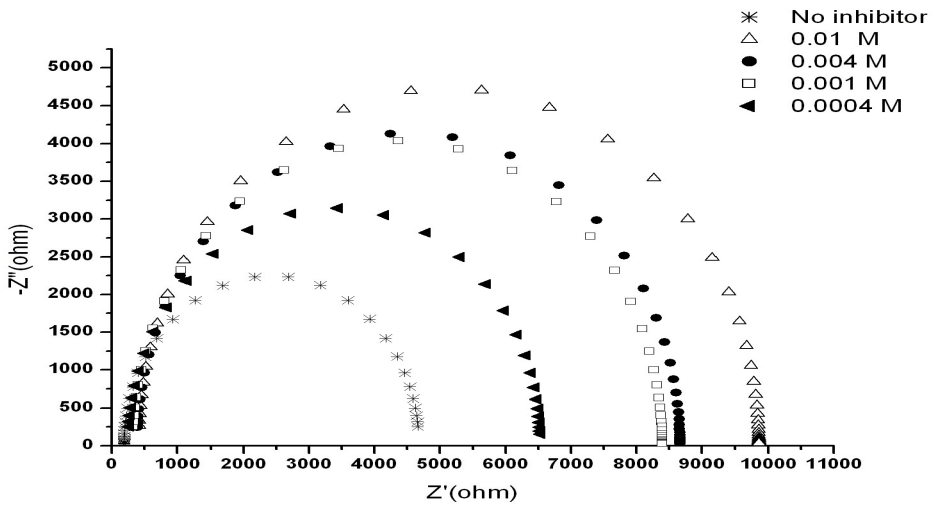


**Figure 4.8** Impedance plot obtained at 25 °C in 1.0 M HCl in various concentration of PMDH.

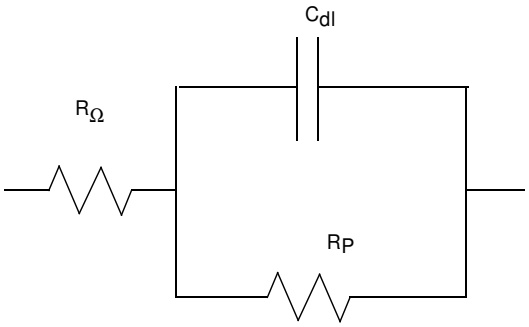


**Figure 4.9** The equivalent circuit model used to fit the experimental results.

Surface coverage value, $\theta$, is a function of inhibitor concentration. The surface coverage values were calculated from following equation [148]:

$$\theta = [1 \quad \frac{R_p}{R_{p(inh)}} \qquad [ \qquad -)$$

Where $R_p$ and $R_{p(inh)}$ are the polarization resistance without and with inhibitor respectively.

**Table 4.4**

Fitting impedance data of aluminum in 1.0 M HCl in absence and presence of different concentrations of PMDH.

| $C$ (M) | $A.R_\Omega$ ($\Omega$ cm$^2$) | $A.R_p$ ($\Omega$ cm$^2$) | $C_{dl}/A$ ($\mu$F/cm$^2$) | $\theta$ | ($IE$ %) |
|---|---|---|---|---|---|
| Blank | 35.99 | 881.162 | 30.76 | — | — |
| 0.01 | 79.48 | 1854.56 | 32.15 | 0.5248 | 52.48 |
| 0.004 | 75.36 | 1624.95 | 31.94 | 0.4577 | 45.77 |
| 0.001 | 62.21 | 1585.70 | 31.69 | 0.4443 | 44.43 |
| 0.0004 | 51.02 | 1234.41 | 31.33 | 0.2861 | 28.61 |

## 4.1.3 SEM technique

**Figure 4.10** shows the aluminum surface after immersion in different concentration of inhibitor. Images show that with increasing PMDH concentration, corrosive surface area decreases

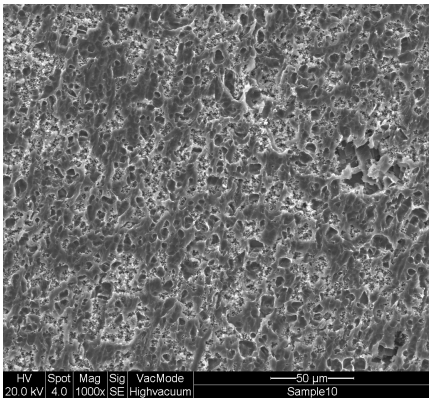


**(a)**

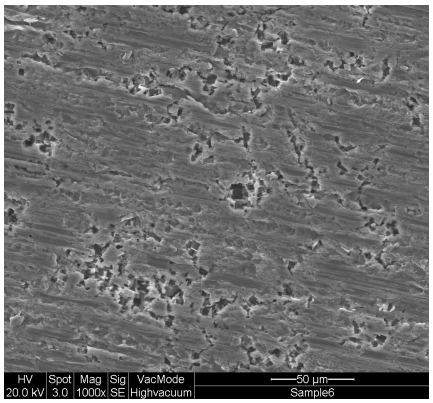


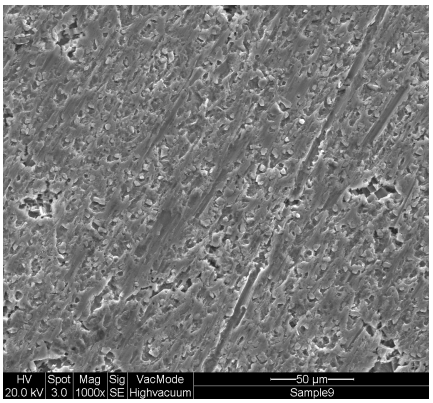


**(b)** **(c)**

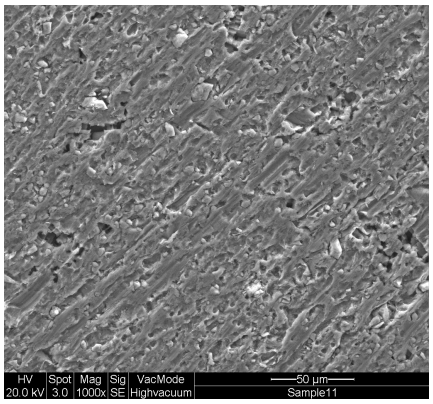


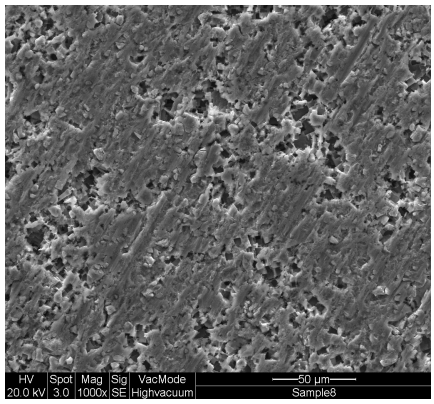


**(d)** **(e)**

**Figure 4.10** SEM images of corroded aluminum surface in blank and different concentration of PMDH: (a) 1.0 M HCl, (b) 0.01 M, (c) 0.004 M, (d) 0.001 M, (e) 0.0004 M.

## .4.2 Effect of Benzene -1, 2, 4, 5-tetracarboxylic dianhydride (PMDH) on aluminum corrosion in 1.0 M NaCl solution

### 4.2.1. Electrochemical impedance spectroscopy

**Figure 4.11** shows the complex impedance plots of the aluminum electrode in the 1.0 M NaCl solution in the absence and presence of PMDH in the concentration range of 0.01 to 0.0004 M at 25 °C. The addition of PMDH did not change the general shape of the semicircles but large increases in their radii are observed with increasing the PMDH concentration. The equivalent circuit shown in **Figure 4.12** was chosen such that it best fitted the observed data.

The parameters calculated from fitting the impedance are listed in **Table 4.5.** The increase of the polarization resistance with the increase in the PMDH concentration is due to decreasing both the general and pitting corrosions. The $C_{dl}$ values tended to decrease despite of polarization resistance, the reason of this decrease was explained in last section **(4.1).**

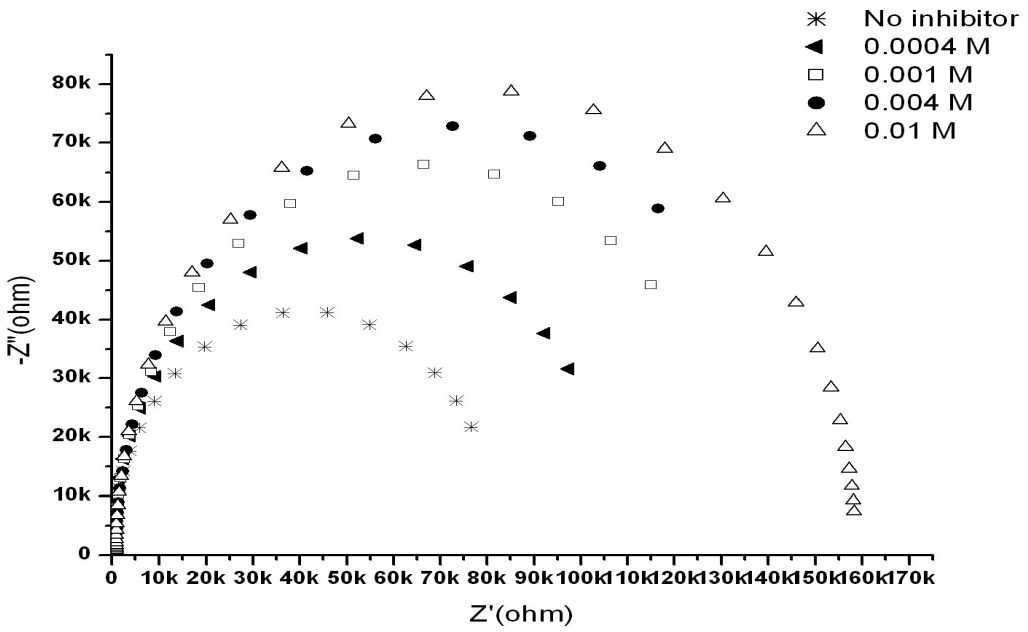


**Figure 4.11** Impedance plot obtained at 25 °C in 1.0 M NaCl in various concentration of PMDH.

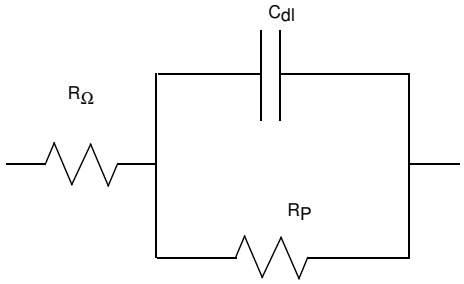


**Figure 4.12** The equivalent circuit model used to fit the experimental results.

**Table 4.5**

Fitting impedance data of aluminum in 1.0 M NaCl in absence and presence of different concentrations of PMDH at 25°C.

| $C$ (M) | $A.R_{\Omega}$ ($\Omega$ cm$^2$) | $A.R_p$ (K$\Omega$ cm$^2$) | $C_{dl}/A$ ($\mu$F/cm$^2$) | $\theta$ | ($IE$ %) |
|---|---|---|---|---|---|
| Blank | 45.17 | 16.27 | 4.72 | — | — |
| 0.01 | 154.64 | 30.97 | 5.56 | 0.4746 | 47.46 |
| 0.004 | 167.40 | 28.57 | 5.43 | 0.4305 | 43.05 |
| 0.001 | 107.15 | 26.06 | 4.80 | 0.3756 | 37.56 |
| 0.0004 | 91.01 | 21.14 | 4.79 | 0.2303 | 23.03 |

#### 4.2.1.1 Effect of temperature

The effect of temperature on the inhibition efficiency of inhibitor in 1.0 M NaCl at temperatures' ranging from 25 to 45 °C was obtained to calculate the thermodynamics parameters. The results are shown in **Table 4.6**. With increasing temperature, polarization resistance ($R_p$), solution resistance ($R_s$) and inhibition efficiency decreases.

It can be due to adsorption of inhibitor' molecules on the aluminum surface. The strength of adsorption process at higher temperatures will decrease and physical adsorption of the inhibitor molecules on the metal surface will happened.

**Figure 4.13 (a-e)** shows the effects of different temperatures on the polarization curves of aluminum in 1.0 M NaCl in the presence and absence of PMDH.

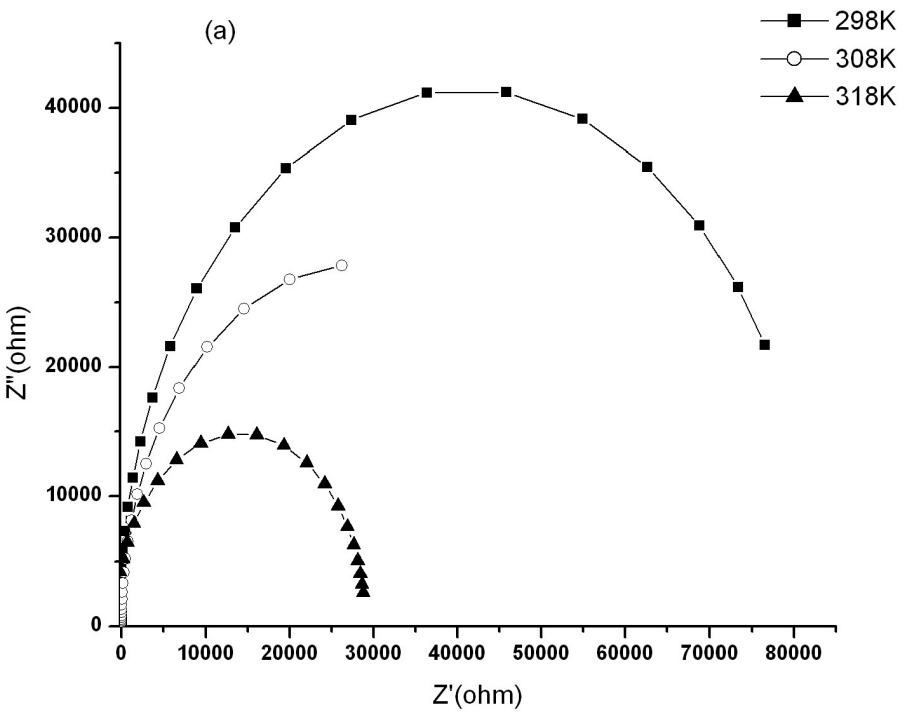

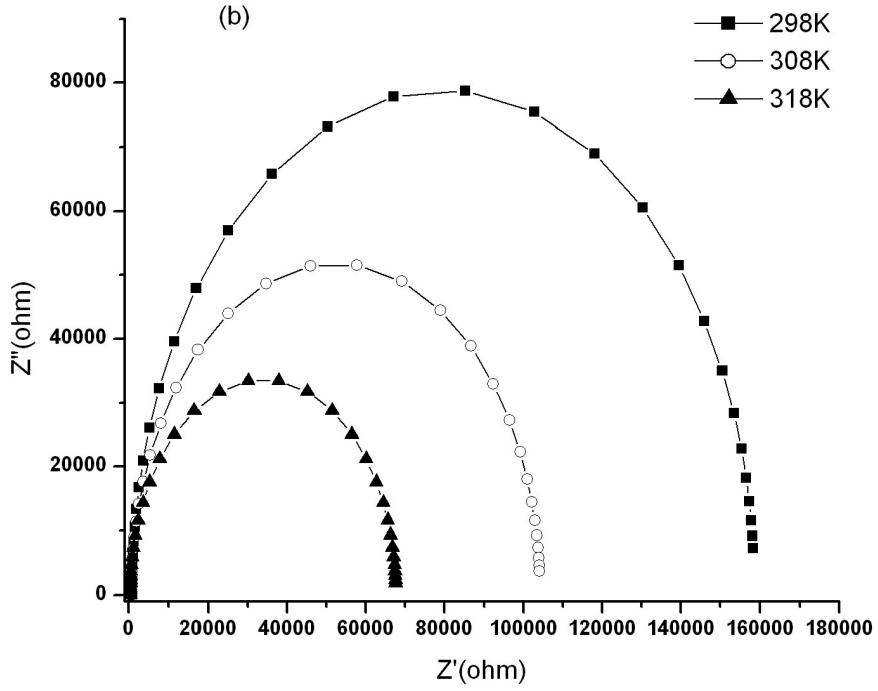
(b)
298K
308K
318K
Z''(ohm)
Z'(ohm)
0
20000
40000
60000
80000
100000
120000
140000
160000
180000

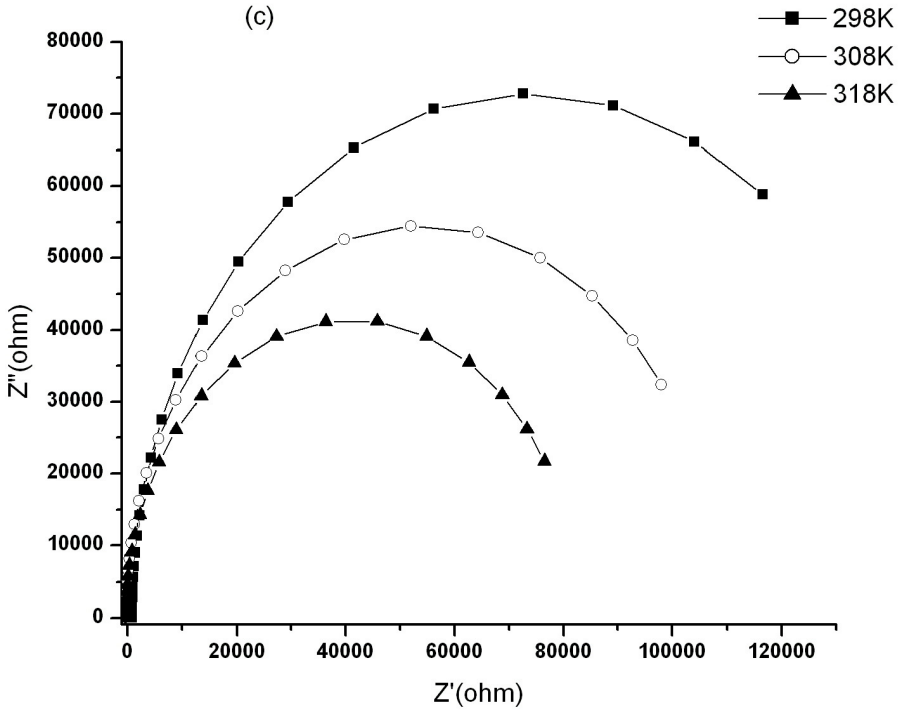
(c)
298K
308K
318K
Z''(ohm)
Z'(ohm)
0
10000
20000
30000
40000
50000
60000
70000
80000
100000
120000

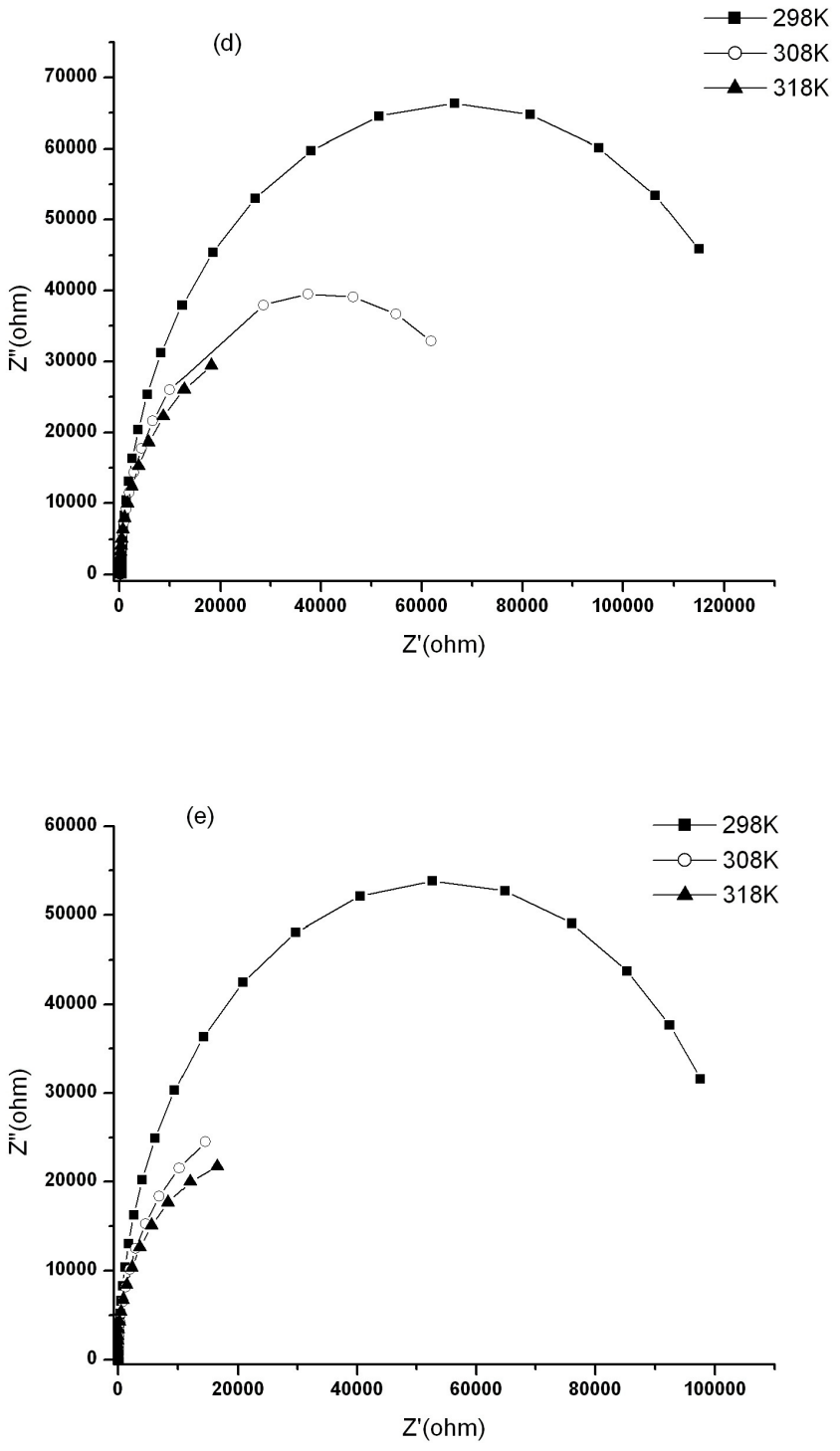


**Figure 4.13** Impedance plots for Al in **(a)** 1.0 M NaCl and in the presence of **(b)** 0.01 M PMDH, **(c)** 0.004 M PMDH, **(d)** 0.001 M PMDH and **(e)** 0.0004 M PMDH at different temperatures.

**Table 4.6**

Fitting impedance data of aluminum in 1.0 M NaCl in absence and presence of different concentrations of PMDH at three different temperatures.

| $C$ (M) | $T$ (K) | $A.R_{\Omega}$ ($\Omega$ cm$^2$) | $A.R_p$ (K$\Omega$ cm$^2$) | $C_{dl}/A$ ($\mu$F/cm$^2$) | $\theta$ | ($IE$ %) |
|---|---|---|---|---|---|---|
| Blank | 298 | 45.17 | 16.27 | 5.43 | — | — |
| | 308 | 15.57 | 13.95 | 4.80 | | |
| | 318 | 13.46 | 11.83 | 4.69 | | |
| 0.01 | 298 | 154.64 | 30.97 | 4.72 | 0.4746 | 47.46 |
| | 308 | 117.16 | 23.33 | 5.51 | 0.4020 | 40.20 |
| | 318 | 69.86 | 19.20 | 6.67 | 0.3638 | 36.38 |
| 0.004 | 298 | 167.40 | 28.57 | 5.56 | 0.4205 | 42.05 |
| | 308 | 58.90 | 21.39 | 4.81 | 0.3218 | 32.18 |
| | 318 | 45.09 | 17.27 | 5.43 | 0.2749 | 27.49 |
| 0.001 | 298 | 107.15 | 26.06 | 4.80 | 0.3556 | 35.56 |
| | 308 | 57.90 | 17.54 | 3.39 | 0.2046 | 20.46 |
| | 318 | 27.10 | 13.95 | 4.94 | 0.1519 | 15.19 |
| 0.0004 | 298 | 91.01 | 21.14 | 4.79 | 0.2303 | 23.03 |
| | 308 | 18.58 | 15.65 | 4.80 | 0.1086 | 10.86 |
| | 318 | 14.52 | 12.81 | 4.60 | 0.0765 | 7.65 |

With reducing inhibitor concentration and increasing temperature a decrease in the inhibition efficiency (*IE* %) is observed; this effect is shown in **Figure 4.14.**

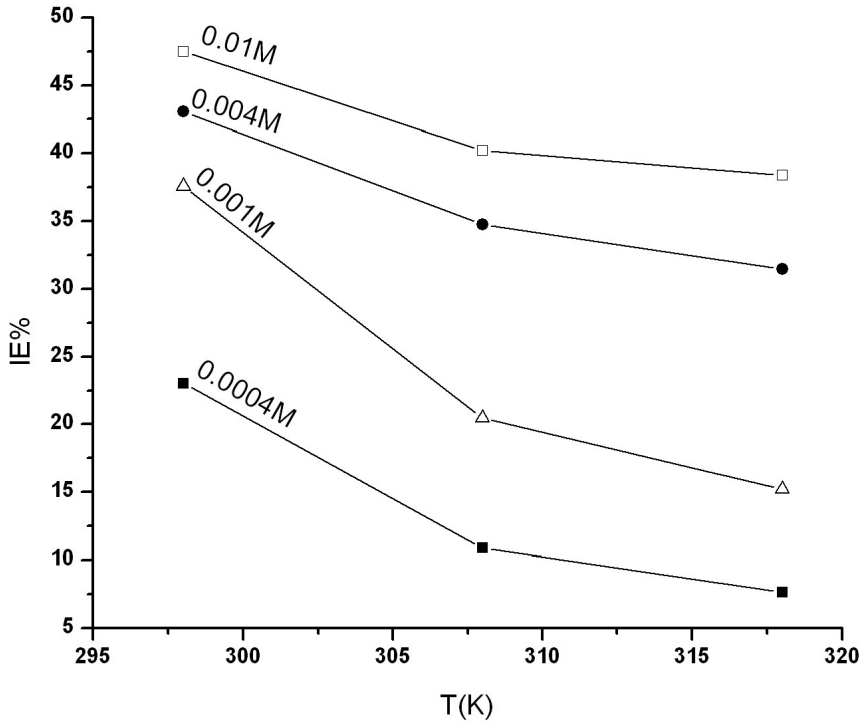


**Figure 4.14** Effect of PMDH on inhibition efficiency of Al corrosion in various concentration and temperatures.

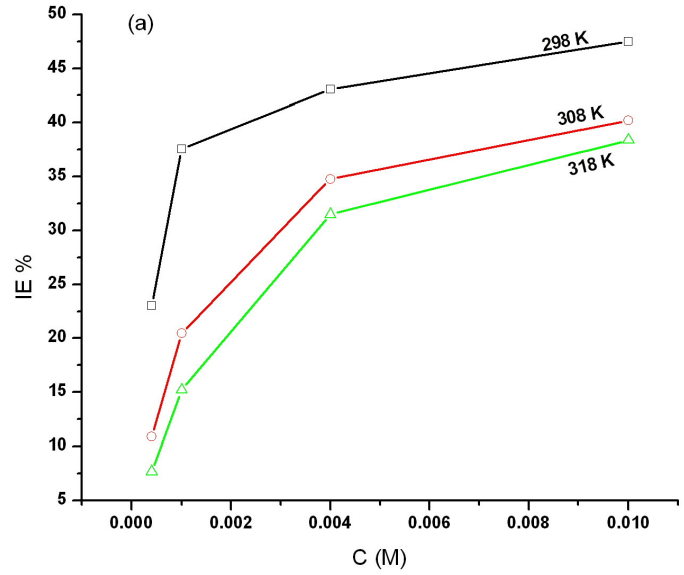


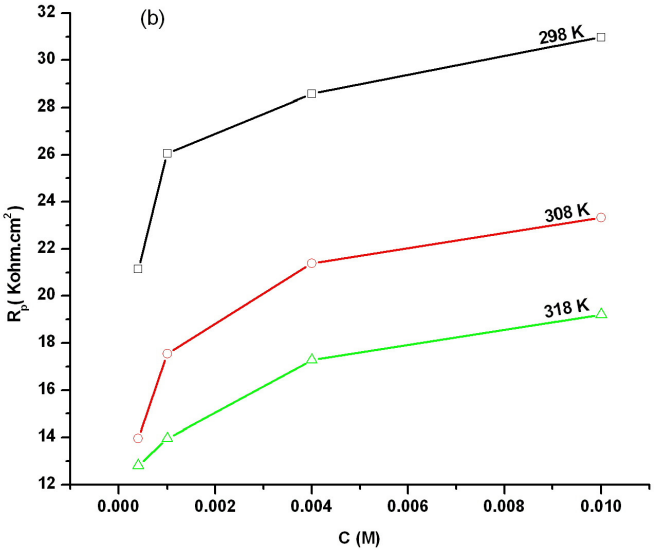


**Figure 4.15** Effect of PMDH concentration on inhibition efficiency **(a)** and on polarization resistance **(b)** of Al corrosion in 1.0 M NaCl at different temperatures.

**Figure 4.15** shows that the inhibition efficiency and polarization resistance increases as the concentrations of the inhibitor increase. These plots in 1.0 M HCl at different temperatures suggest that the inhibitor protect the dissolution of aluminum in 1.0 M NaCl solution.

#### 4.2.1.2 Adsorption isotherm

The plot of log ($\theta$/1- $\theta$) versus log $C$ for different concentrations of PMDH in three temperatures is given in **Figure 4.16.** The values of surface coverage ($\theta$) of different concentrations of PMDH obtained from the impedance plots in the temperature ranges (25 - 45 $^{o}$C) have been used.

The Langmuir adsorption isotherm assumes that there are no interaction or repulsion forces between the adsorbed molecules.

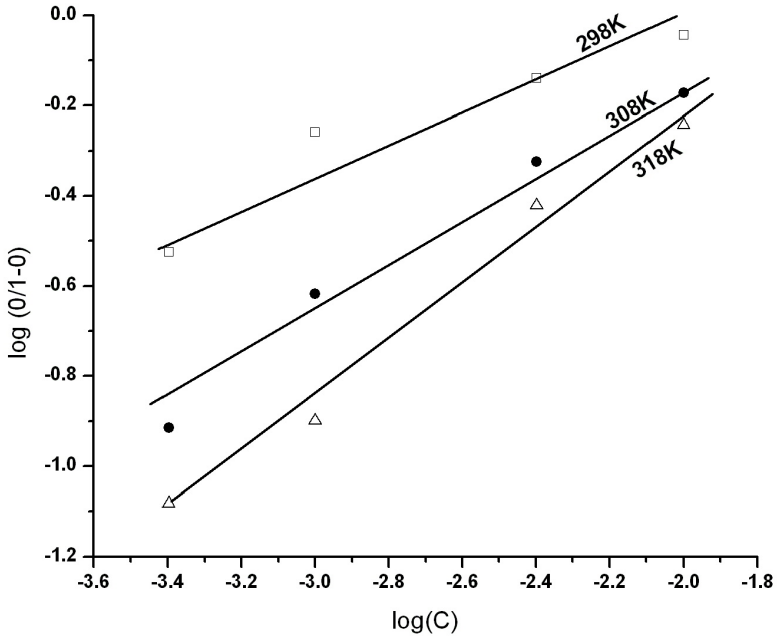


**Figure 4.16** Plot of Langmuir adsorption isotherm of PMDH obtained by using surface coverage values calculated by electrochemical impedance spectroscopy at different temperatures.

## 4.2.2 SEM technique

**Figure 4.17** shows the aluminum surface after immersion in different concentration of inhibitor. Images show that with increasing PMDH concentration, corrosive surface area decreases.

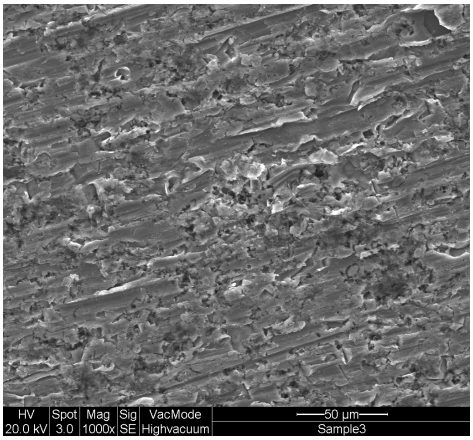


**(a)**

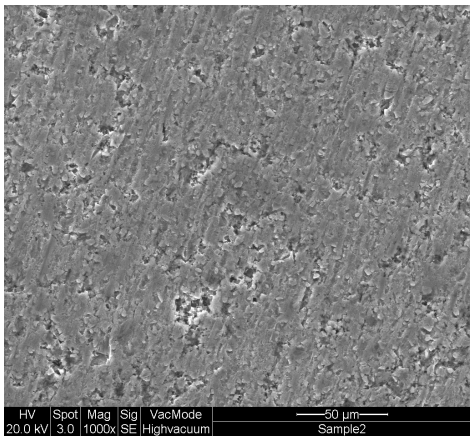


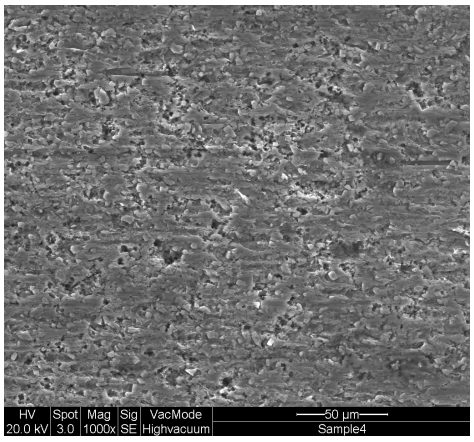


**(b)** **(c)**

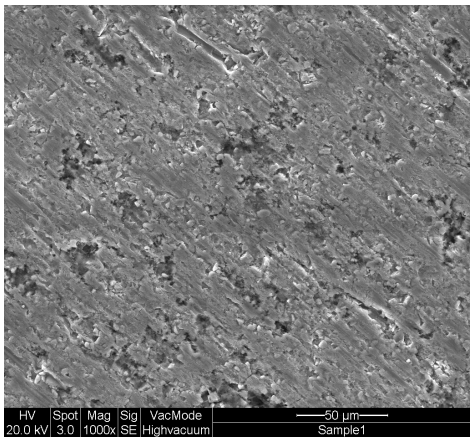


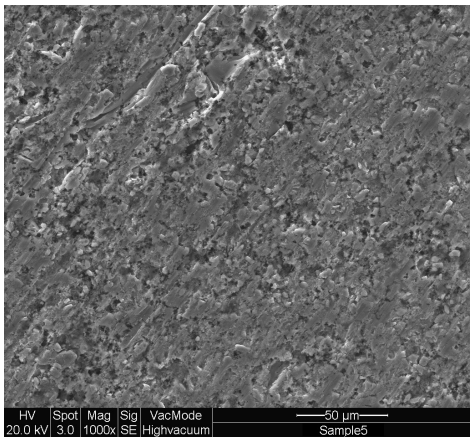


**(d)** **(e)**

**Figure 4.17** SEM images of corroded aluminum surface in blank and different concentration of PMDH: **(a)** 1.0 M NaCl, **(b)** 0.01 M, **(c)** 0.004 M, **(d)** 0.001 M, **(e)** 0.0004 M.

## 4.3 Effect of Benzene -1, 2, 4, 5-tetracarboxylic dianhydride (PMDH) on aluminium corrosion in 1.0 M KOH solution

### 4.3.1. Electrochemical impedance spectroscopy

**Figure 4.18** shows a typical Nyquist plots for pure Al in 1.0 M KOH solution containing different concentrations of PMDH at 25 °C. The impedance spectra consists of a large capacitive semi-circle at HF (high frequency) and an inductive semi-circle at intermediate frequencies (IF), followed by a second capacitive semi-circle at LF (low frequency) values. The HF capacitive semi-circle is attributed to the presence of a protective oxide film covering the surface of Al. The (IF) inductive loop may be related to the relaxation process obtained by adsorption PMDH molecules into the oxide film. The second capacitive loop observed at LF values could be assigned to the metal dissolution [154,155 ]. The impedance parameters derived from Nyquist plots are given in **Table 4.7**.

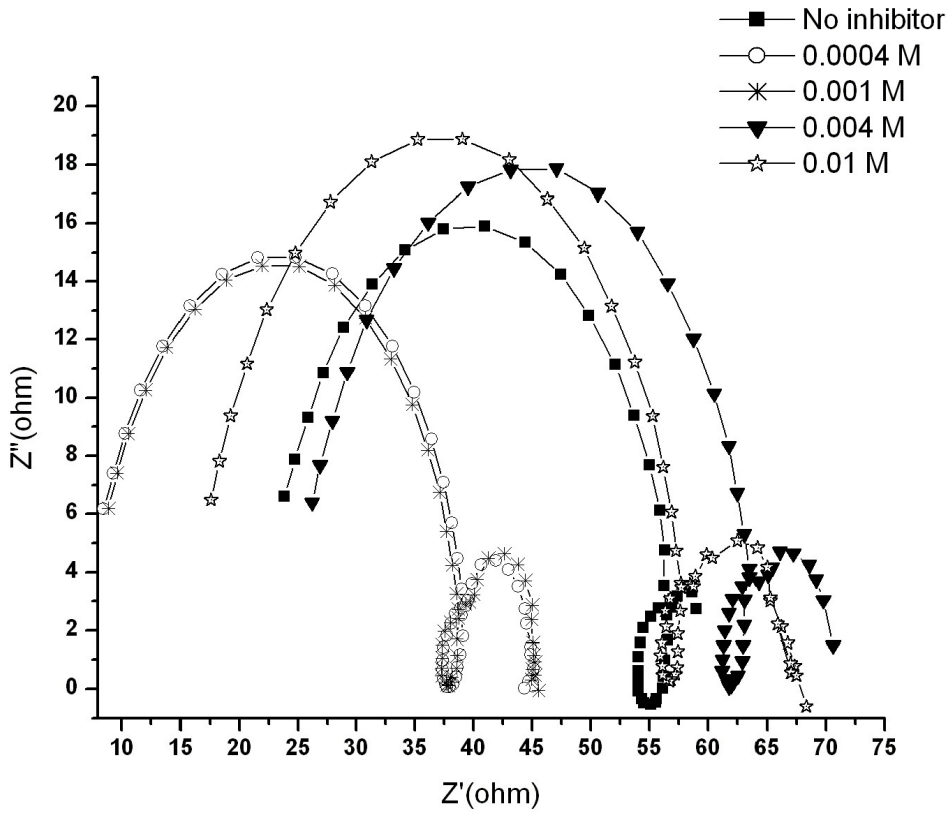


**Figure 4.18** Nyquist plots obtained at 25 ºC in 1.0 M KOH in various concentration of PMDH.

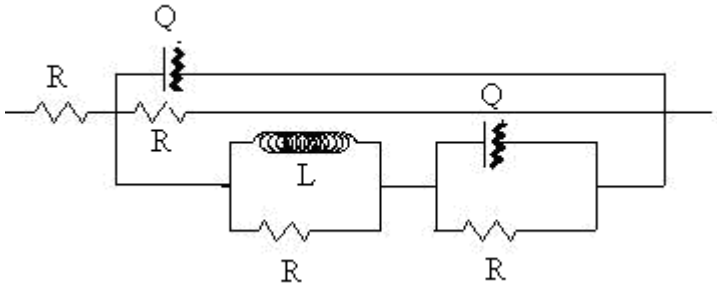


[R ((QR)[(RL)(RQ)])]

**Figure 4.19** The equivalent circuit model used to fit the experimental results.

**Table 4.7**

Fitting impedance data of aluminum in 1.0 M KOH in absence and presence of different

concentrations of PMDH.

| $C$ (M) | $R_\Omega$ ($\Omega$) | $A.R_p$ ($\Omega$ cm$^2$) | $\theta$ | ($IE$ %) |
|---|---|---|---|---|
| Blank | 4.10 | 6.50 | — | — |
| 0.01 | 22.85 | 9.16 | 0.291 | 29.12 |
| 0.004 | 16.40 | 7.75 | 0.162 | 16.20 |
| 0.001 | 10.15 | 6.91 | 0.060 | 6.00 |
| 0.0004 | 5.60 | 6.81 | 0.046 | 4.61 |

#### 4.3.1.1 Effect of temperature

The effect of temperature on the inhibition efficiency of inhibitor in 1.0 M KOH at temperatures' ranging from 25 to 45 °C was obtained to calculate the thermodynamics parameters (see **Figure 4.20**). The results are shown in **Table 4.8** with increasing temperature, polarization resistance ($R_p$) and inhibition efficiency decreases.

It can be due to adsorption of inhibitor' molecules on the aluminum surface. The strength of adsorption process at higher temperatures will decrease and physical adsorption of the inhibitor molecules on the metal surface will happen.

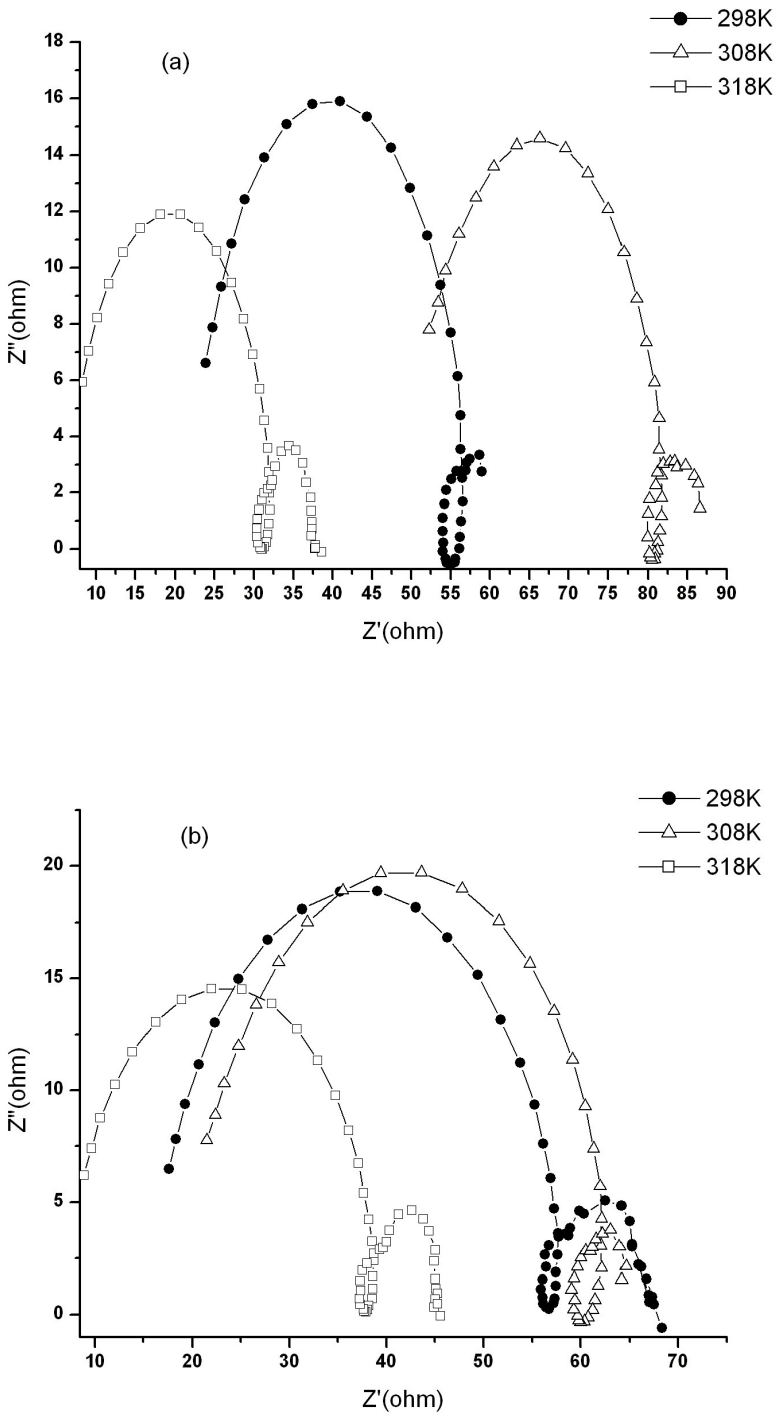


**Figure 4.20 (a and b)** The effect of different temperatures on the polarization curves of aluminum in 1.0 M KOH in the presence and absence of 0.01 M PMDH.

**Table 4.8**

Fitting impedance data of aluminium in 1.0 M KOH in absence and presence of 0.01 M of PMDH at three different temperatures.

| $C$ (M) | $T$ (K) | $A.R_p$(KΩ cm$^2$) | $\theta$ | ($IE$ %) |
|---|---|---|---|---|
| Blank | 298 | 6.50 | — | — |
| | 308 | 6.32 | — | — |
| | 318 | 5.61 | — | — |
| 0.01 | 298 | 9.16 | 0.291 | 29.12 |
| | 308 | 4.58 | 0.217 | 21.65 |
| | 318 | 3.77 | 0.188 | 18.75 |

The dependence of inhibition efficiency and polarization resistance on temperature and concentrations of the inhibitor in **Figure 4.21 (a-c)** is observed**.**

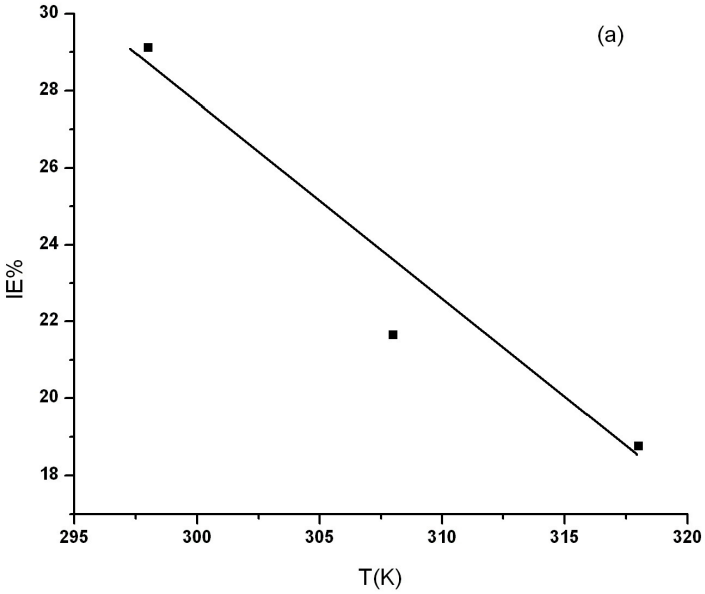
(a)
IE%
T(K)
30
28
26
24
22
20
18
295
300
305
310
315
320

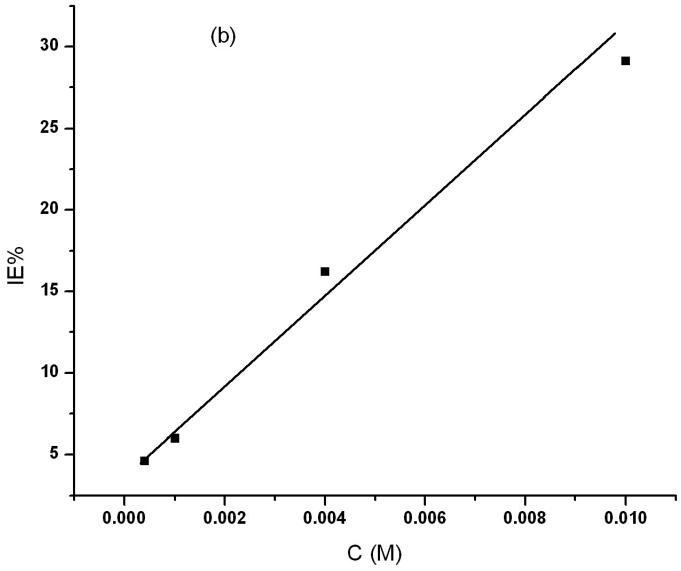
(b)
IE%
C (M)
30
25
20
15
10
5
0.000
0.002
0.004
0.006
0.008
0.010

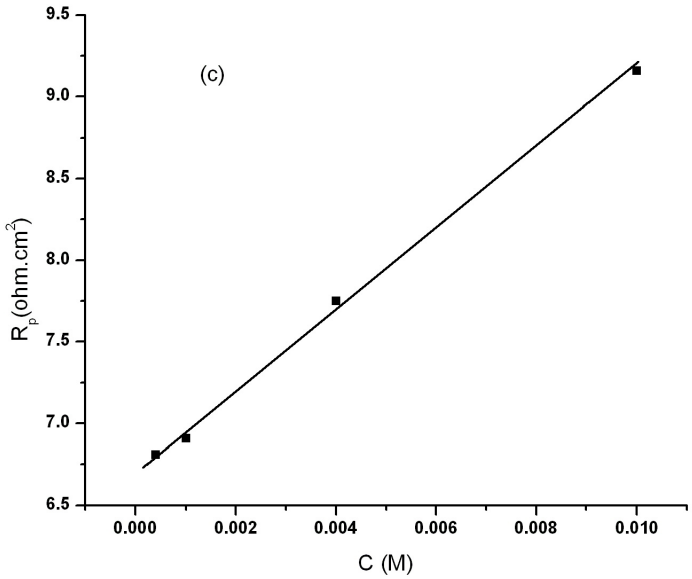


**Figure 4.21** Effect of temperature **(a)**, concentrations **(b)** on inhibition efficiency and polarization resistance of Al corrosion in presence of PMDH **(c)**.

## 4.3.2 SEM technique

**Figure 4.22** shows the aluminum surface after immersion in different concentration of inhibitor. Images show that with increasing PMDH concentration, corrosive surface area decreases.

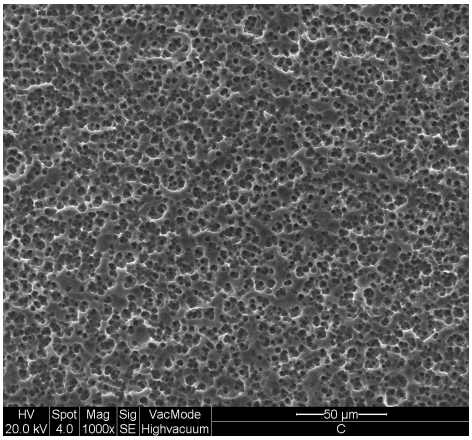


**(a)**

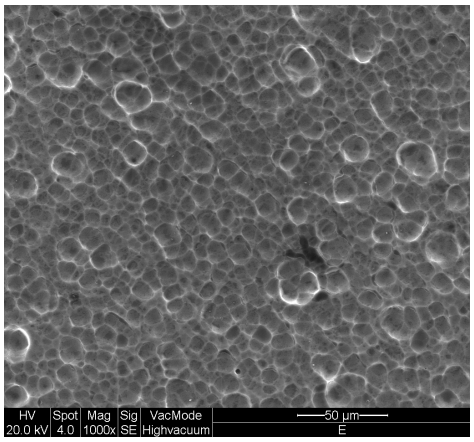


**(b)**

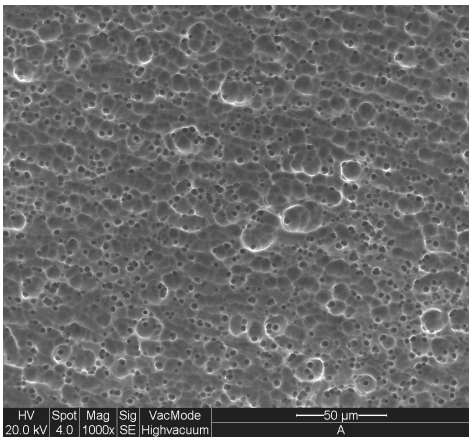


**(c)**

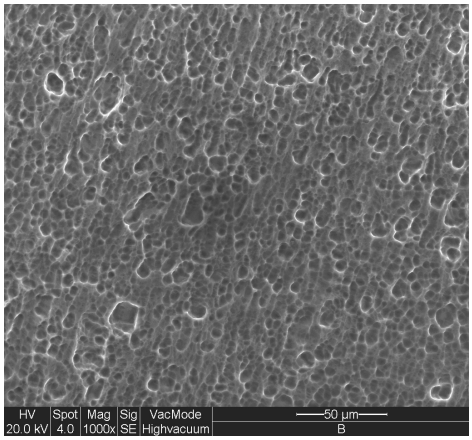


**(d)**

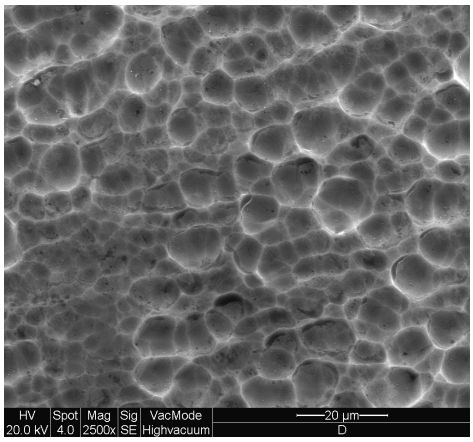


**(e)**

**Figure 4.22** SEM images of corroded aluminum surface in blank and different concentration of PMDH: **(a)** 1.0 M KOH, **(b)** 0.01 M, **(c)** 0.004 M, **(d)** 0.001 M, **(e)** 0.0004 M.

# PART 2

# Theoretical Studies

## 4.4 Structure of inhibitor molecule

It is expected that the inhibitor molecules in solution behave differently from that in vacuum. The solvent effect on molecular structure of solute can be studied by a model which is known as polarized continuum model (PCM) [156-158]. In this model, the solvent is treated as a continuum dielectric media and the solute considered as a trapped molecule in a cavity surrounded by solvent.

This theoretical work is based on the isolated inhibitor model [159,160] i.e., the substrate and environmental factors (e.g., substrate, solvent, and electric field in electric double layer [EDL] have been totally ignored. The Gaussian 03 suite of programs and Gausview 3.0 were used for all calculations.

Electronic and spatial molecular structure of an inhibitor can be related to its effectiveness. The interactions metal-inhibitor can be influenced by some certain quantum-chemical parameters, such as the HOMO (highest occupied molecular orbital) energy that is often associated with the capacity of a molecule to donate electrons, the LUMO energy and the dipole moment.

Electronic chemical potential ($\mu$) and molecular hardness ($\eta$) are two important factors, through which the inhibitory action can be investigated [12, 32]. These quantities are defined as follows:

$$\mu = 1/2\,(IP + EA)$$

$$\eta = 1/2\,(IP - EA)$$

In these relations, *IP* and *EA* are ionization potential and electron affinity, respectively, and their values can be approximately equal to negative values of the (HOMO) and lowest unoccupied molecular orbital (LUMO) energy levels:

$$IP = -E_{HOMO}$$

$$EA = -E_{LUMO}$$

The chemical interaction of inhibitor molecules with the metal surface is possible only after the migration of the molecules from the bulk of solution to the metal/solution interface. For this reason, the chemical potential ($\mu$), and molecular hardness ($\eta$) of PMDH were calculated using the B3LYP method with the 6-311G** basis set.

The theoretical parameters related to the molecular electronic structure are presented in the following table.

**Table 4.9**

Calculated quantum parameters of PMDH using B3LYP/6-311G** method.

| ***IP*** **(eV)** | ***EA*** **(eV)** | **Dipole moment (Debye)** | **Chemical potential ($\mu$)** | **Hardness ($\eta$)** | **Inhibitor** |
|---|---|---|---|---|---|
| -0.33154 | -0.48164 | 0.0048 | -0.406 | 0.075 | PMDH In basic media |
| 0.28552 | 0.09862 | 4.6009 | 0.192 | 0.093 | PMDH In acidic media |

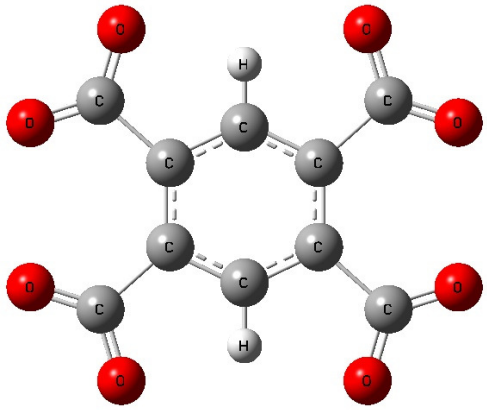
O
O
C
H
C
C
C
C
C
C
C
O
O
C
O
O
C
H
O
O

**(a)**

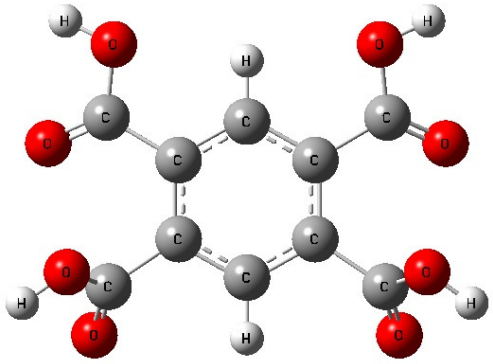

**(b)**

**Figure 4.23** Optimized structure of PMDH molecule in **(a)** basic and **(b)** acidic media by using the B3LYP/6-311G** method.

It can be seen from (**Figure 4.23**), that the PMDH molecule in 1.0 M KOH is planar and in 1.0 M HCl its shape is different and this difference in structure can affect the adsorption process. Values of the net charge density on the aromatic ring in acidic media (-0.1719) and basic media (-0.6022) show that there could be a relationship between the inhibition efficiency (IE) and the net charges on aromatic rings. Charges and dipole moments were calculated by using Mulliken analysis method [161]. It is possible that the negative charges on oxygen (O) atoms of PMDH in 1.0 M KOH induces extra negative charge on the aromatic ring and as a result the net charge on oxygen (O) atoms decreases.

As the adsorption of inhibitor molecules is through lone pair electrons of the oxygen atoms [123-125], and there is a correlation between inhibition efficiencies and power of inhibitor molecule; therefore, with the reduction in charge on the oxygen atoms, the efficiency of the oxygen atoms will decrease and results in *IE* for 1.0 M KOH is less than 1.0 M HCl solution.

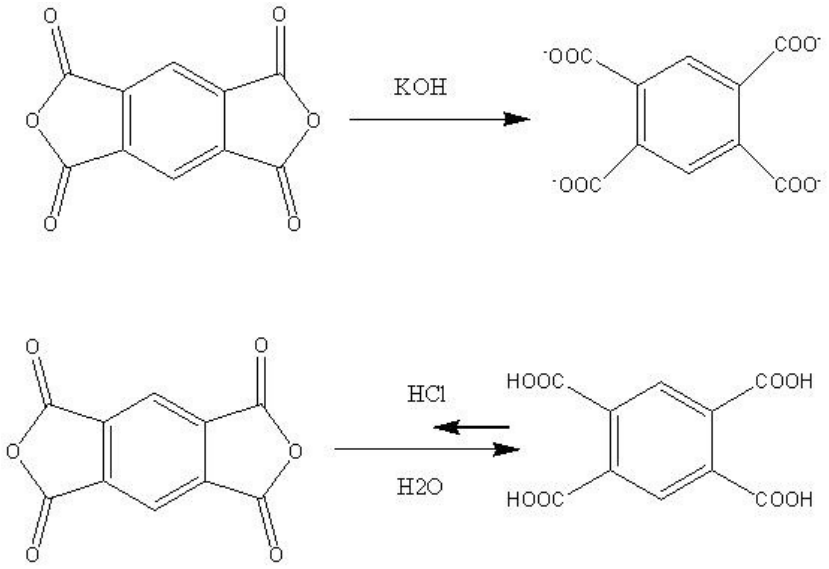


**Figure 4.24** PMDH structures in acidic and basic media.

The HOMO energy can indicate the disposition of the molecule to donate electrons to an appropriate acceptor with empty molecular orbital. Increase in the values of $E_{HOMO}$ can affect on the adsorption and therefore the inhibition efficiency [162,163]. The obtained values of $E_{HOMO}$ corresponding to the inhibitor in the two media are quite different. This indicates different in capacity for charge donation to the metallic surface. The corrosion rate is expected to decrease with increase in HOMO energy [164]; therefore an increase in the corrosion inhibition may be observed.

The good correlation of $\mu$ with inhibition efficiency can be related to the fact that any factor causing an increase in chemical potential would enhance the electronic releasing power of inhibitor molecule. The amounts of hardness in both media are very similar and it seems that this parameter does not play a sufficient role to account for the variation in the experimental inhibition efficiencies.

# 5. CONCLUSION

Benzene -1, 2, 4, 5-tetracarboxylic dianhydride (PMDH) shows good corrosion inhibition property against aluminum corrosion in the acid and basic media from EIS measurements and polarization curves. EIS measurements gave the decrease of $C_{dl}$ with the increase in inhibitor concentrations, which can be explained by increased adsorption of the inhibitor on the aluminium surface which displaces the adsorbed $H_3O^+$ and $Cl^-$ ions. The inhibition efficiency (*IE %*) decreased with increasing temperature as a result of higher desorption of the inhibitor from the aluminum surface. An increase in temperature will tend to stimulate corrosive attack by increasing the rate of electrochemical reactions and diffusion processes and lead to a higher corrosion rate. The efficiency increased when the concentration increased for all temperatures because the corrosion current density and corrosion rate decrease and polarization resistance increases. Adsorption of this inhibitor on the aluminum surface can be closely modeled to the Langmuir isotherm that assumes there are no interaction or repulsion forces between the adsorbed molecules. The negative values of $\Delta G_{ads}$ show that the adsorption is spontaneous and the activation energy decrease with addition of inhibitor's concentration. The SEM images show the retarding of aluminum corrosion in acids solution by this inhibitor.

The inhibition efficiency of studied inhibitor increases when $E_{HOMO}$ decreases, dipole moment and charge of O atoms acts as active centers for adsorption process increase. The values of free energy of adsorption and the relationship between the inhibition efficiency values, thermodynamic data and calculated quantum chemistry parameters suggest that PMDH is adsorbed on aluminium surface by physical mechanism.

# References


[1] Rey A., (dir.).(1993). *Dictionnaire historique de la langue francaise*. Le Robert, Paris.

[2] Z. Ahmad. (2006). *Principles of Corrosion Engineering and corrosion control*. Elsevier Science & Technology Books. Publ. (p. 2-8)

[3] C. Vargel. (2004). *Corrosion of Aluminium*: Elsevier, Oxford. (p. 81, 98, 113, 386, 387 and 398).

[4] V. S Bagotsky. (2006). *Fundamentals of electrochemistry*. 2nd edn. New Jersey: John Wiley & Sons. (p. 45,110)

[5] L. L. Shreir, R. A. Jarman, G.T. Burstein. (1994). *Corrosion*. 3rd edn. Butterworth Heinemann Press. (p.1,16)

[6] P. M. Aziz, and Godard, H. P. (1956). *Corrosion*. **(12)**. (p. 495)

[7] E. Deltombe., Pourbaix M. (1956). *Comportement e´lectrochimique de l'aluminium, diagramme d'e´quilibre tension pH du syste`me Al_ H2O a` 25 °C*. Cebelcor. Rapport technique. **(42).**

[8] J.C. Scully. (1975), *the fundamentals of corrosion*, 2nd edn. vol. 17, Pergamon International, Oxford, International serious of monographs on materials science and technology.

[9] R. Rosliza, W. B. Wan Nik, H.B. Senin, Mater. (2008). *Journal. Chem. Phys*. **(107)**. 281

[10] S.E. Frers, M.M. Stefenel, C. Mayer, T. Chierchie. (1990). *Journal Applied. Electrochem*. **(20).** 996

[11] I.L. Rozenfeld. (1981)**.** *Corrosion Inhibitors*. New York: Mac Graw-Hill. (p. 182)

[12]A. Kolics, A. S. Besing, P. Baradlai, R. Haasch, A. Wieckowski.(2001). *Journal. Electrochem. Society*. **(148)**. 251

[13] M. Pourbaix. (1966). *Atlas o Electrochemical Equilibria in aqueous Solutions*. New York: Pergamon Press.

[14] E. M. Sherif, S.M. Park. (2006). *Journal. Electrochim. Acta*.**(51)**. 1313

[15] A. M. Abdel- Gaber, B. A Abd-El-Nabey, I. M. Sidahmed, A. M. Elzayady, M. Saadawy. (2006). *Mater. Chem. Phys*. **(98)**. 291

[16] F. Bentiss, M. Largenee, M. Tralsnel. (1999). *Journal. Appl. Electroch*. **(29)**. 1073

[17] T.Y. Soror, H.A. El-Dahan, N.G. El-Sayed Ammer. (1999). *Journal. Mater. Sci. Technol*. **(15)**. 16

[18] H.B. Fan, C.Y. Fu, H.L. Wang, X.P. Guo, J.S. Zheng. (2002). *Br. Corrosion Journal*. **(37)**. 122

[19] N. Hackerman, J.D. Sudbury. (1950). *Journal Electrochem Society*. **(94)**. 4

[20] N. Hackerman. (1962). *Corrosion*. **(18)**. (p. 332).

[21] E.M. Sherif, S.-M. Park. (2005). *Journal Electrochem Society*. **(152)**. 205

[22] C. Monticelli, G. Brunoro, A. Frignani, F. Zucchi. (1991). *Corrosion Science*. **(32)**. 693

[23] N.A. Ogurtsov, A.A. Pud, P. Kamarchik, G.S. Shapoval. (2004). *Synth. Met*. **(14).** 43

[24] D. Zhu, W.J. van Ooij. (2003). *Corrosion Science*. **(45)**. 2163

[25] D. Zhu, W.J. van Ooij. (2003). *Corrosion Science*. **(45)**. 2177

[26] S. Doulami, K. Beligiannis, Th. Dimogerontakis, V. Ninni, I. Tsangaraki Kaplanoglou. (2004). *Corrosion Science*. **(46)**. 1765

[27] A.Y. El-Etre.(2001). *Corrosion Science*. **(43)**. 1031

[28] H. Ashassi-Sorkhabi, S.A. Nabavi-Amri. (2000). *Acta Chim. Slov*. **(47).** 587

[29] E.E. Ebenso.( 2002). *Mater. Chem. Phys*. **( 71)**. 62

[30] E.E. Ebenso, U.J. Ekpe, B.I. Ita, E.O. Offiong, U.J. Ibok. (1999). *Mater. Chem. Phys*. **( 60)**. 80

[31] E.S. Ferreria, C. Giacomelli, F.C. Giacomelli, A. Spinelli.(2004)**.** *Mater. Chem. Phys.* **(83).** 129

[32] S.B. Saidman, J.B. Bessone. (2002). *J. Electroanal. Chem*. **(521)**. 87

[33] S.S.A. Rehim, H.H. Hassan, M.A. Amin.(2002). *Appl. Surf. Sci.* **(187)**. 279

[34] A.A. El-Shafei, S.A. Abd El-Maksoud, A.S. Fouda. (2004). *Corrosion Science*. **(46)**. 579

[35] R. Ambat, E.S. Dwarakodasa. (1994). *J. Appl. Electrochem*. **(24)**. 911

[36] W.M. Carroll, C.B. Breslin.(1991). *J. Br. Corros*. **(26)**. 225.

[37] R. Ambat, E.S. Dwarakodasa. (1994). *J. Appl. Electrochem*. **(24)**. 911

[38] Gulbransen E.A., Wysong W.S., Thin oxyde film on aluminum. (1947). *Journal of Physic and Colloid Chemicals.* **(51)**. 1087–1103

[39] Mott N.F. (1939). *Theory of the formation of protective oxides films on metals.* (p. 143)

[40] Tolley G. ( 1950). The oxide film on aluminum. Consideration of experimental facts. *Metal Industry*. **(77)**. (p. 255–258)

[41] Hunter M.S., Fowle P. (1956). Natural and thermally oxide films on aluminum. *Journal of the Electrochemical Society*. **(103)**. (p. 482–485)

[42] J. OM. Bockris, Y. Kang. (1997). *J. Solid State Electrochem*. **(1)**. 17

[43] M.M. Mazhar, W.A. Badawy, M.M. Abou-Romia. (1987). *Surf. Coat. Technol*. **(29)**. 337

[44] R.T. Foley, T.H. Nguyen. (1982). J. *Electrochem. Soc*. **(129)**. 464

[45] L. Tomcsanyi, K. Varga, I. Bartik, G. Horanyi, E. Maleczki. (1989). *Elecrochim. Acta* .**(34)**. 855

[46] W.A. Badawy, F.M. Al-Kharafi, A.A. El-Azab. (1999). *Corros. Sci*. **(41)**. 709

[47] F. Hunkeler, G.S. Frankel, H. Bohni. (1987). *Corrosion.* **(43).** 189

[48] N. Sato. (1995). *Corros. Sci.* **(37)**. 1947

[49] S. Berrada, M. Elboujdaini, E. Ghali. (1994). *J. Appl. Electrochem*. **(24)**. 911

[50] F.D. Bogar, R.T. Foley. (1972). *J. Electrochem. Soc*. **(119)**. 462

*Transactions of the Faraday Society*. **(35)**. 1175–1177

[51] E. E. Oguzie, B. N. Okolue, E. E. Ebenso, G. N. Onuohaa, A. I. Onuchukwu. (2004). *Mater.Chem. Phys*. **(87)**. 394

[52] A. A. Awady, B. A. Abd-El-Nabey, S.G. Aziz. (1993). *J. Chem. Soc*. **(84)**. p. 795

[53] Gregory J.N., Hodge N., Iredale J.V.J. (1956). *The static corrosion of nickel and other materials in molten caustic soda.* England: Atomic Energy Research Establishment Harwell.

[54] Dmitruk B.F., Zarutbitskii O.G., Babich N.N.(1983). *Ukraine Khim. Zh*. **(49)**. 690-693

[55] H.U.V Vogel. (1940). *Korrosionsverhalten von Aluminium und Aluminium legierungen gegen wa¨ßrige Lo¨sungen verschiedener Temperaturen, Korrosion und Metallschutz*. **(16)**. (p. 259–278).

[56] Brown A.P., Battles J.E. (1987). The corrosion of metals and alloys by sodium polysulfides melts at 350 ºC. *Proceedings of the Electrochemical Society*. 237–246

[57] Horst R.L., Binger W.W. (1961). Corrosion studies of aluminium in chemical process operations. *Corrosion*. **(17)**. (p. 25–30).

[58] I.N Putilova., S.A Balezin., V.P Barranik. (1960). *Metallic Corrosion Inhibitors*. Oxford: Pergamon Press. (p.155–170)

[59] L. Young. (1961). *Anodic Oxide Films*. New York: Academic Press. (p. 4–9).

[60] B. Muller, G. Kubitzki, G. Kinet. (1998). *Corros. Sci*. **(40).** 1469

[61] L. Garrigues, N. Pebere, F. Dabosi. (1996). *Electrochim. Acta*. **(41)**. 1209

[62] G.T. Hefter, N.A. North, S.H. Tan. (1997). *Corrosion*. **(53)**. 657

[63] E. Khamis. (1990). *Corrosion*. **(46)**. 476

[64] L. Bazzi, S. Kertit, M. Hamani, Bull. (1998). *Electrochem*. **(14)**. 34

[65] S.S. Mahmoud, Bull. (1995). *Electrochem*. **(11)**. 366

[66] D. Brasher, A. Kingsbury. (1958). *Trans. Faraday Soc*. **(54)**. 1214

[67] J.B. Lusdem, S. Szklarska, Z. (1978). *Corros*. **(34)**. 169

[68] B.R.W. Hinton, D.R. Arnott, Ryan. (1986). *Mater. Forum*. **(9)**. 162

[69] F. Mansfeld, S. Lin, S. Kim, H. Shih. (1987). *Corros. Sci*. **(27)**. 997

[70] D.D. Macdonald. (1993). *Electrochem. Soc*. **(138)**. 27

[71] M. Bethencourt, F.J. Botana, J.J. Calvino, M. Marcos, M.A. Rodriguez. (1998). *Corros. Sci.* **(40)**. 1803

[72] Y. Dud, R. Govea-Rueda, M. Galicia. (2005). *J. Phys. Chem. B*. **(109)**. 2674.

[73] V.S. Sastry.(1998). *Corrosion Inhibitors. Principles and Applications*. New York: John Wiley & Sons.

[74] M. Bouayed, H. Rabaa, A. Srhiri, J.-Y. Saillard, A. Ben Bachir, A. Le Beuzed. (1999). *Corros. Sci*. **(41)**. 501

[75] M. Bouayed, H. Rabaa, A. Srhiri, J.Y. Saillard, A. Ben Bachir. (1999). *Corros. Sci*. **(41)**. 501

[76] A.Y. El-Etre. (2003). *Corros. Sci*. **(45)**. 2485

[77] N. Subramanyan, A.R. Yamuna, Brit. (1969). *Corros. J*. **(4)**. 32

[78] N. Subramanyan, V. Kapali, S. Venkitakrishna Iyer. (1971). *Corros. Sci*. **(11)**. 115

[79] G. Daufin, J.P. Labbe, J. Pagetti. (1977). *Corros. Sci*. **(17)**. 901

[80] K.B. Sarangapani, V. Balaramachandran,V. Kapali, S. Venkatakrishna Iyer, M.G. Potdar, K.S. Rajagopalan. (1984). *J. Appl. Electrochem*. **(14)**. 475

[81] H.B. Shao, J.M. Wang, Z. Zhang, J.Q. Zhang, C.N. Cao. (2001). *Corrosion*. **(57)**. 577

[82] T. Hovarth, E. Kalman. (1993). *Progress in the Understanding and Prevention of Corrosion.* (p. 923)

[83] E.E. Ebenso. (2002). *Mater. Chem. Phys*. **(71)**. 62

[84] E.E. Ebenso, U.J. Ekpe, B.I. Ita, E.O. Offiong, U.J. Ibok. (1999). *Mater. Chem. Phys*. **(60)**. 80

[85] A.M. Al-Mayouf. (1996). *Corros. Prev. Control*. **(6)**. 68

[86] E.E. Ebenso, P.C. Okafor, U.J. Ekpe, Bull. (2002). *Electrochem.* **(18)**. 551

[87] A. Aytac, U. Ozmen, M. Kabasakaloglu. (2005). *Mater. Chem. Phys*. **(89)**. 176

[88] B. Mernari, H. El Attari, M. Traisnel, F. Bentiss, M. Lagrenée. (1998). *Corros. Sci.* **(40)**. 391

[89] F. Bentiss, M. Lagrenée, M. Traisnel, J.C. Hornez. (1999). *Corros. Sci.* **(41)**. 789

[90] E.E. Ebenso, U.J. Ekpe, B.I. Ita, E.O. Offiong, U.J. Ibok. (1999). *Mater. Chem. Phys.* **(60)**. 80

[91] E.S. Ferreria, C. Giacomelli, F.C. Giacomelli, A. Spinelli. (2004). *Mater. Chem. Phys.* **(83)**. 129

[92] S.B. Saidman, J.B. Bessone. (2002). *J. Electroanal. Chem*. **(521)**. 87

[93] E.E. Ebenso, U.J. Ekpe, B.I. Ita, E.O. Offiong, U.J. Ibok. (1999). *Mater. Chem. Phys.* **(60)**. 80

[94] E.S. Ferreira, C. Giacomelli, F.C. Giacomelli, A. Spinelli. (2004). *Mater. Chem. Phys*. **(83)**. 129

[95] S.M. Beloglazow. (1993). *Progress in the Understanding and Prevention of Corrosion. 2.Institute of Materials*. (p. 908)

[96] M.N. Dessai, M.B. Dessai, C.B. Shah, S.M. Dessai. (1986). *Corros. Sci*. **(26)**. 827

[97] S.A. Abd El-Maksoud. (2002). *Corros. Sci*. **(44)**. 803

[98] M. Ajmal, A.S. Mideen, M.A. Quraishi. (1994). *Corros. Sci*. **(36)**. 79

[99] J.M. Abdel Kader, A.M. Shams El Din, (1970). *Corros. Sci*. **(10)**. 551

[100] Y. Abboud, A. Abourriche, T. Saffaj, M. Berrada, M. Charrouf. (2006). *Appl. Sur. Sci.* **(252)**. 8178

[101] S.S. Sampat, J.C. Vora. (1974). *Corros. Sci*. **(14)**. 591

[102] T.L. Barr. (1977). *J. Vac. Sci. Technol*. **(14)**. 660

[103] J.W. Diggle, T.C. Downie, C.W. Goulding. (1969). *Chem. Rev*. **(65)**. 365

[104]Bavarian, B. (2000). STE rebar in concrete. *Corrosion inhibitors*. USA: Newsletter, Cortec Corporation. (p. 1-4)

[105] C.M.A. Brett. (1990). *J. Appl. Electrochem*. **(20)**. 1000

[106] S. L. Chawla. R. K. Gupta. (1993). *Material Selection for Corrosion Control, ASM International*. Ch. 25.

[107] L. Bazzi, S. Kertit, M. Hamani. (1998). *Bull. Electrochem*. **(14)**. 34

[108] S.S. Mahmoud. (1995). *Bull. Electrochem*. **(11)**. 366

[109] D. Brasher, A. Kingsbury. (1958). *Trans. Faraday Soc*. **(54)**. 1214.

[110] J.B. Lusdem, S. Szklarska, Z. (1978). *Corrosion*. **(34)**. 169

[111] B.R.W. Hinton, D.R. Arnott, Ryan. (1986). *Mater. Forum*. **(9)**. 162

[112] F. Bentiss, M. Lagrenee, M. Traisnel, J.C. Hornez. (1999). *Corros. Sci*. **(41)**. 789

[113] F. Bentiss, M. Traisnel, M. Lagrenee. (2001). *J. Appl. Electrochem*. **(31)**. 41

[114] M.A. Quraishi, R. Sardar. (2002). *Mater. Chem. Phys*. **(78)**. 425

[115] L.M. Rodriguez-Valdez, A. Martinez-Villafane, D. Glossman-Mitnik. (2004). *J. Mol. Struct. (THEOCHEM)*. **(681)**. 83- 88

[116] S. Bilgic, M. Sahin. (2001). *Mater. Chem. Phys*. **(70)**. 290

[117] M.N. Dessai, M.B. Dessai, C.B. Shah, S.M. Dessai. (1986). *Corros. Sci*. **(26)**. 827

[118] S.A. Abd El-Maksoud. (2002). *Corros. Sci*. **(44)**. 803

[119] Oakes B.D. (1981). Historical review inhibitors mechanisms, *NACE Corrosion*. No. 248.

[120] I. Lukovits, E. Kalman, F. Zucchi. (2001). *Corrosion*. **(57)**. 3

[121] F. Touhami, A. Aouniti, Y. Abed, B. Hammouti. (2000). *Corros. Sci*. **(42)**. 929

[122] L. Tang, X. Li, L. Li, G. Mu, G. Liu. (2006). *Surf. Coat. Technol*. **(201)**. 384

[123] A.B. Tadros, A.B. Abdenabery. (1988). *J Electroanal.Chem*. **(24)**. 433

[124] J.G.N. Thomas. (1980). Some new fundamental aspects in corrosion inhibition. *Proceedings, 5th Eur. Symp. Corros. Inhibitors*. Italy: Ferrara. (p. 453)

[125] O.L. Riggs Jr. (1973). *Corrosion Inhibitors*, 2nd edn. C.C. Nathan, Houston, TX,

[126] Lorenz, W. J. and Mansfeld, F. (1981). *Corrosion Science*. **(9)**. 647

[127] J. B. Foresman, A. Frisch. (1996). *Exploring Chemistry with Electronic Structure Methods.* 2nd edn. (p. 3, 7, 97- 99).

[128] M. R. Arshadi, M. Lashgari, Gh. A. Parsafar. (2004). *Mater. Chem. Phys*. **(86)**. 311

[129] M. Lashgari, M. R. Arshadi, Gh.A. Parsafar. (2005). *Corrosion (NACE).* **(61)**. 778

[130] M. Lashgari, M.R. Arshadi, Gh.A. Parsafar, V. S. Sastri. (2006). *Corrosion (NACE).* **(62)**. 199

[131] M. Baerns, R. Imbihl, V.A. Kondratenko, R. Kraehnert, W.K. Offermans, R.A. van Santen, A. Scheibe. (2005). *J. Catal*. **(232)**. 226

[132] M. Lashgari, M. R. Arshadi, V. S. Sastri. (2007). *J. Electrochem. Soc*. **(154)**. 93

[133] A. Nilsson, L. G .M. Pettersson, J. K. Nørskov. (2008). *Chemical Bonding at Surfaces and Interfaces.* Amsterdam: Elsevier.ch. 4.

[134] L.H. Thomas. (1927). *Proc. Camb. Phil. Soc*. **(23)**. 542; E. Fermi. (1927). *Rend. Accad.Lincei.* **(6)**. 602

[135] H. Hohenberg, W. Kohn. (1964). *Phys. Rev. B.* **(136)**. 864

[136] W. Kohn, L. (1965). *J. Sham, Phys. Rev. A*. **(140)**. 1133

[137] E. Fermi, Rend. (1927). *Accad. Lincei*. **(6)**. 602

[138] A. D. Becke. (1986). *J. Chem. Phys*. **(84)**. 45240.

[139] A. D. Becke. (1988). *Phys. Rev. A*. **(38)**. 3098

[140] J. P.Perdew. (1986). *Phys. Rev. B*. **(33)**. 8822

[141] J. P. Perdew. (1986). *Phys. Rev. B*. **(34)**. 7406

[142] J. P. Perdew,Y. Wang. (1986). *Phys. Rev. B*. **(33)**. 8800

[143] C. Lee, W. Yang, R. G. Parr.(1988). *Phys. Rev. B.* **(37)**. 785

[144] J.P. Perdew, K. Burke, M. Ernzerhof.(1996). *Phys. Rev. Lett*.**(77)**. 3865

[145] A. D. Becke. (1993). *J. Chem. Phys*. **(98)**. 5648

[146] B. El Mehdi, B. Mernari, M. Trainsel, F. Bentiss, M. Lagrenee. (2002). *Mater. Chem. Phys. (***77**). 489

[147] H. Ashassi-Sorkhabi, B. Shaabani, D. Seifzadeh.( 2005). *Appl. Surf. Sci*. **(239)**. 154

[148] M.S. El- Basiouny, A.S. Babaqi, R.M. Abdulla, Bull. (1990). *Electrochem*. **(6)**. 909.

[149] G. Trabanelli, C. Montecelli, V. Grassi, A. Frignani. (2005). *J. Cem. Concr. Res*. **(35)**. 1804

[150] M.S. Morad. (2000). *Corros. Sci*. **(42)**. 1313

[151] F. Bentiss, M. Lagrenee, M. Traisnel, J.C. Hornez. (1999). *Corros. Sci*. **(41)**. 789

[152] W. H. Li, Q. He, C. L. Pei, B. R. Hou. (2007). *Electrochim. Acta* **(52)**. 6386

[153] F. Mansfeld. (1981). *Corrosion*. **(36)**. 301

[154] S.S. Abd El- Rehim, H.H. Hassan, M.A. Amin. (2001). *Mater. Chem. Phys*. **(70).** 64

[155] M. Gojic, R. Horvat, M. Metikos- Hukovic. **(1995)**. *Proceedings of the Eighth European Symposium on Corrosion Inhibitors (8 SEIC).* (p. 97).

[156] F. Jensen. (2007). *Introduction to Computational Chemistry*. England: John Wiley & Sons Ltd. Ch. 5.

[157] E. Cances, B. Mennucci, J. Tomasi. (1997). *J. Chem. Phys*. **107 (8).** 3032

[158] M. Lashkari, M. R. Arshadi. (2004). *Chem. Phys*. **(299)**. 131

[159] J. Fang, J. Li. (2002). *J. Mol. Struct. (Theochem.)*. **(593)**. 179

[160] N. Khalil. (2003). *Electrochim. Acta.* **(48)**. 2,635

[161] I. N. Levine. (1991). *Quantum Chemistry*, 4th edn. NJ: Prentice-Hall, Upper Saddle River. Ch. 13 and 15.

[162] N. Khalil.(2003). *Electrochimica Acta Journal*. **(48)**. 2635

[163] I. Lukovits, K. Pa´lfi, I. Bako´, E. Ka´lma´n. (1997). *Corrosion*. **(53)**. 915

[164] V.S. Sastri, J.R. Perumareddi.(1997). *Corrosion Science*. **(53)**. 617